AMPKα1 Regulates Macrophage Skewing at the Time of Resolution of Inflammation during Skeletal Muscle Regeneration.

Rémi Mounier, Marine Théret, Ludovic Arnold, Sylvain Cuvellier, Laurent Bultot, Olga Göransson, Nieves Sanz, Arnaud Ferry, Kei Sakamoto, Marc Foretz, et al.

▶ **To cite this version:**

Rémi Mounier, Marine Théret, Ludovic Arnold, Sylvain Cuvellier, Laurent Bultot, et al.. AMPKα1 Regulates Macrophage Skewing at the Time of Resolution of Inflammation during Skeletal Muscle Regeneration.. Cell Metabolism, 2013, 18 (2), pp.251-64. 10.1016/j.cmet.2013.06.017 . inserm-00857933v2

HAL Id: inserm-00857933

https://inserm.hal.science/inserm-00857933v2

Submitted on 18 Sep 2018

HAL is a multi-disciplinary open access archive for the deposit and dissemination of scientific research documents, whether they are published or not. The documents may come from teaching and research institutions in France or abroad, or from public or private research centers.

L'archive ouverte pluridisciplinaire **HAL**, est destinée au dépôt et à la diffusion de documents scientifiques de niveau recherche, publiés ou non, émanant des établissements d'enseignement et de recherche français ou étrangers, des laboratoires publics ou privés.

HAL
archives-ouvertes.fr

AMPKα1 Regulates Macrophage Skewing at the Time of Resolution of Inflammation during Skeletal Muscle Regeneration.

Rémi Mounier, Marine Théret, Ludovic Arnold, Sylvain Cuvellier, Laurent Bultot, Olga Göransson, Nieves Sanz, Arnaud Ferry, Kei Sakamoto, Marc Foretz, et al.

▶ **To cite this version:**

Rémi Mounier, Marine Théret, Ludovic Arnold, Sylvain Cuvellier, Laurent Bultot, et al.. AMPKα1 Regulates Macrophage Skewing at the Time of Resolution of Inflammation during Skeletal Muscle Regeneration.: AMPKα1 regulates macrophage skewing. Cell Metab, 2013, 18 (2), pp.251-64. <10.1016/j.cmet.2013.06.017>. <inserm-00857933>

HAL Id: inserm-00857933
http://www.hal.inserm.fr/inserm-00857933

Submitted on 4 Sep 2013

HAL is a multi-disciplinary open access archive for the deposit and dissemination of scientific research documents, whether they are published or not. The documents may come from teaching and research institutions in France or abroad, or from public or private research centers.

L'archive ouverte pluridisciplinaire **HAL**, est destinée au dépôt et à la diffusion de documents scientifiques de niveau recherche, publiés ou non, émanant des établissements d'enseignement et de recherche français ou étrangers, des laboratoires publics ou privés.

Graphical Abstract

Click here to download Graphical Abstract: Grafical abstract Mounier D-13-00308R1.docx

Mounier Cell Metabolism D-13-00308R1

Graphical abstract

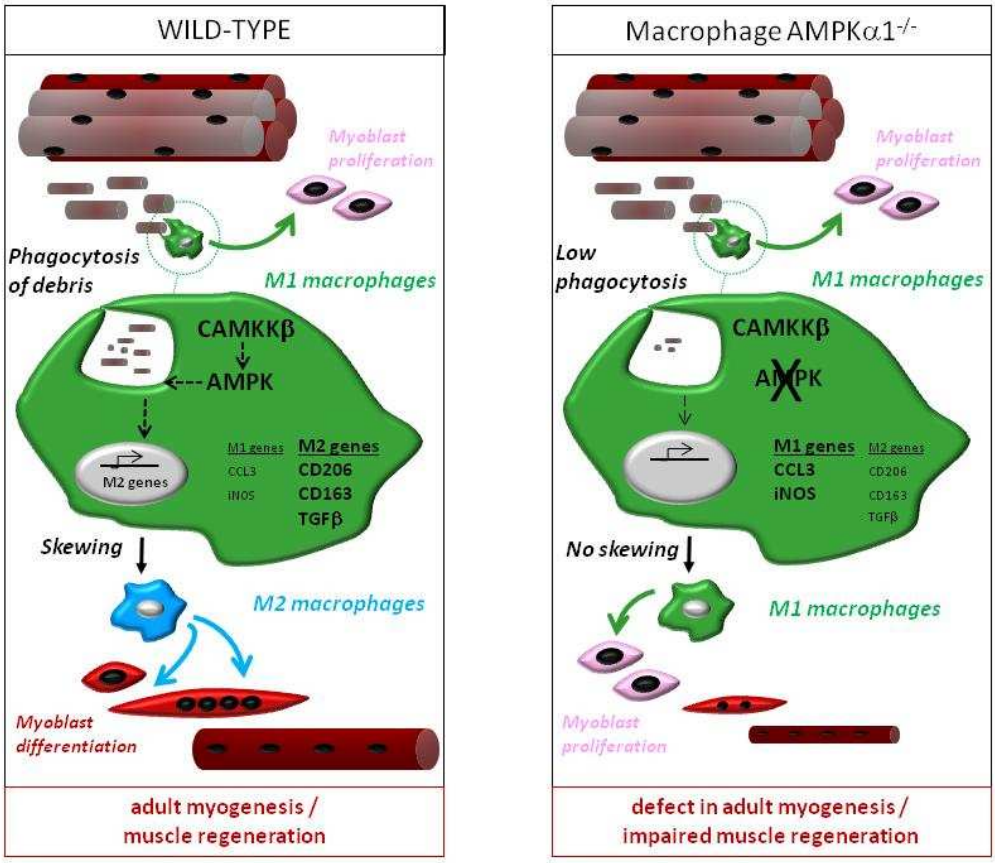

*Manuscript
Click here to view linked References

AMPKα1 regulates macrophage skewing at the time of resolution of inflammation during skeletal muscle regeneration

Rémi Mounier[1,2,3,9], Marine Théret[1,2,3,9], Ludovic Arnold[4,5], Sylvain Cuvellier[1,2,3], Laurent Bultot[6], Olga Göransson[7], Nieves Sanz[1,2,3], Arnaud Ferry[3,8], Kei Sakamoto[6], Marc Foretz[1,2,3], Benoit Viollet[1,2,3,10], Bénédicte Chazaud[1,2,3,10]

1 INSERM, U1016, Institut Cochin, Paris, France

2 CNRS, UMR8104, Paris, France

3 Université Paris Descartes, Sorbonne Paris Cité, France

4 INSERM, UMR_S945, Faculté de médecine Pitié Salpétrière, Paris, France

5 Université Pierre et Marie Curie, France

6 Nestlé Institute of Health Sciences SA, Lausanne, Switzerland

7 Department of Experimental Medical Sciences, Lund University, Lund, Sweden

8 Institut de Myologie, Université Pierre et Marie Curie, Sorbonne Universités, Paris, France

Corresponding author:

Bénédicte Chazaud

Institut Cochin

INSERM U1016 - CNRS 8104 - Université Paris Descartes

24, Rue du Faubourg Saint Jacques

75014 Paris

Tel: (33) 1 44 41 24 63

Tel: (33) 1 44 41 24 12

benedicte.chazaud@inserm.fr

Foonotes

9 These authors contributed equally to this work

10 These authors contributed equally to this work

Short title : AMPKα1 regulates macrophage skewing

SUMMARY

Macrophages control the resolution of inflammation through the transition from a pro-inflammatory (M1) to an anti-inflammatory (M2) phenotype. We present here evidence for a role of ~~describe a novel function of~~ AMPKα1, a master regulator of energy homeostasis, in macrophage skewing that occurs during skeletal muscle regeneration. Muscle regeneration was impaired in AMPKα1$^{-/-}$ mice. *In vivo* loss-of-function (LysM-Cre;AMPKα1$^{fl/fl}$ mouse) and rescue (bone-marrow transplantation) experiments showed that macrophagic AMPKα1 was required for muscle regeneration. Cell-based experiments revealed that AMPKα1$^{-/-}$ macrophages did not fully acquire the phenotype nor the functions of M2 cells. *In vivo*, AMPKα1$^{-/-}$ leukocytes did not acquire expression of M2 markers during muscle regeneration. Skewing from M1 toward M2 phenotype upon phagocytosis of necrotic/apoptotic cells was impaired in AMPKα1$^{-/-}$ macrophages and when AMPK activation was prevented by inhibition of its upstream activator CaMKKβ. In conclusion, AMPKα1, is crucial for phagocytosis-induced macrophage skewing from pro- to anti-inflammatory phenotype at the time of resolution of inflammation.

INTRODUCTION

The inflammatory response is a spatially and temporally coordinated process. The pro-inflammatory mechanisms initiated and amplified at the onset of the inflammatory response must be controlled to avoid excessive tissue damage. Macrophages play important roles in the resolution of inflammation (Mosser and Edwards, 2008; Lawrence and Fong, 2010). While the first steps of the inflammatory response are associated with pro-inflammatory (M1) macrophages, which secrete pro-inflammatory compounds, resolution of inflammation is associated with M2 macrophages exhibiting an anti-inflammatory phenotype (Mosser and Edwards, 2008). Both *in vitro* and *in vivo* studies have demonstrated that macrophages can undergo dynamic transitions between M1 and M2 states of activation, which is called polarization skewing (Mosser and Edwards, 2008; Lawrence and Fong, 2010). Different regulatory pathways have recently been associated with either the M1 or the M2 activation states. They involve a variety of molecular machineries, at the genomic, transcriptomic and post-transcriptomic levels (reviewed in (Lawrence and Natoli, 2011)). ~~For instance, STAT signaling is involved in the M1 (STAT1) and M2 (STAT6) polarization, whereas different Interferon Regulatory Factors (IRFs) are associated with M1 (IRF5) and M2 (IRF4) gene expression; some molecular systems have been shown to be associated with the expression of the M2 phenotype by macrophages, such as PPARs (particularly PPARγ) and the CREB-C/EBP axis. At the DNA level, promoters of some genes characterizing macrophage inflammatory profile are specifically associated with histone demethylases or nucleosome remodeling complexes. Finally, by controling the stability and translation of mRNAs, post-transcriptional regulons allow the coordinated expression of chemokines and cytokines involved in the initiation as well as the resolution phases of inflammation~~. Despite these recent advances, the signaling pathways involved in regulating the skewing of the macrophage from M1 to M2 phenotype are poorly understood.

AMP-activated protein kinase (AMPK), which is composed of a catalytic (α) and two regulatory (β and γ) subunits, senses the cellular energy levels as forms of ADP/ATP and AMP/ATP ratios. An extensive amount of literature has been published on its roles in the regulation of a multitude of

metabolic processes that maintain cellular energy homeostasis (reviewed in (Hardie, 2011)). Beside these functions, it has recently been reported that enhanced AMPK activation is associated with a decrease of the inflammatory response. Most of the published work was completed in the context of bacterial infection, *i.e*. upon bacterial lipopolysaccharide (LPS) stimulation. Both genetic and pharmacological blocking of AMPK resulted in an enhanced pro-inflammatory response, while AMPK activation decreases the secretion of pro-inflammatory factors by macrophages *in vitro* (Jeong et al., 2009; Peairs et al., 2009; Sag et al., 2008; Zhao et al., 2008; Giri et al., 2004). *In vivo*, administration of AICAR (5-amino-1-β-D-ribofuranosyl-imidazole-4-carboxamide), a pharmacological AMPK activator, attenuates LPS-induced acute lung injury (Zhao et al., 2008) while its inhibition leads to the opposite effect (Xing et al., 2013). These data show that AMPK activity is associated with a decreased pro-inflammatory status of macrophages. However, its role in the acquisition of an anti-inflammatory or M2 status has not been investigated nor has its role in the regulation of the inflammatory profile of macrophages during the resolution of inflammation.

In the present study, we address the role of AMPKα1 in macrophages, the sole AMPKα catalytic unit isoform expressed in these cells (Sag et al., 2008), during skeletal muscle regeneration. After an injury, skeletal muscle regenerates *ad integrum* due to the properties of the satellite cells, the main adult muscle stem cells. It has been shown that macrophages accompany this process by sequentially adopting at least two main inflammatory profiles (Arnold et al., 2007; Saclier et al., 2013). Soon after injury, muscle-associated macrophages exhibit a pro-inflammatory profile and stimulate myogenic precursor proliferation. From 24 to 72h later, these macrophages skew into anti-inflammatory/M2 macrophages that stimulate terminal differentiation of myogenic precursor cells, their fusion into myotubes and the growth of the new regenerating myofibers (Arnold et al., 2007). Thus, post-injury skeletal muscle regeneration provides an excellent paradigm to study events related to the resolution of inflammation. For the present study, we used various genetic mouse models and culture setups, both *in vivo* and *in vitro,* to explore the role of macrophagic AMPKα1 at the time of resolution of inflammation.

RESULTS

AMPKα1 is required for skeletal muscle regeneration

Skeletal muscle regeneration after *i.m*. injection of cardiotoxin (CTX) provides a useful model for sterile inflammation. It provides an homogenous damage in the whole muscle (Suppl. Fig.1A) and triggers the infiltration of a great number of monocytes/macrophages in the regenerating muscle until the end of the repair (Suppl. Fig.1B) (Arnold et al., 2007; Sun et al., 2009). In the CX3CR1$^{GFP/+}$ mouse, monocyte/macrophage subsets can be traced by the GFP label together with the LY6C/G (Gr1) label (Geissmann et al., 2003) (Arnold et al., 2007). The kinetics of AMPKα1 activity during skeletal muscle regeneration (Fig.1A) paralleled the curve of macrophage appearance into regenerating muscle (Fig.1B), with a pronounced increase (+107%, $p>0.001$) from the time of injury to day 2-4, then a decline after day 4. Evaluation of AMPKα1 activity in isolated macrophages confirmed the increase in AMPKα1 activity at day 4 (+135%) (Fig.1C). AMPKα2 activity was very low when compared with normal muscle in wild-type (WT) and AMPKα1$^{-/-}$ mice (Fig.1D). AMPKα1 being the unique catalytic subunit expressed in macrophages (Sag et al., 2008), we explored its role during muscle regeneration. The post injury regeneration process induced by CTX in the *tibialis anterior* (TA) muscle follows a sequence of well-characterized events (Fig.1E). The first phase (1-7 days) includes necrosis of the myofibers, invasion of the injured area by inflammatory cells (neutrophils rapidly followed by macrophages), proliferation of myogenic precursor cells (MPCs), phagocytosis of damaged myofibers by macrophages and differentiation of MPCs. A second phase (7-14/21 days) includes continuation of MPC differentiation, formation, then growth of new myofibers, which are characterized by the central location of their nuclei.

~~Skeletal muscle regeneration was analyzed in AMPKα1$^{-/-}$ *vs.* AMPKα1$^{+/+}$ wild-type (WT) *tibialis anterior* (TA) muscle.~~ Histological analysis shows that skeletal muscle repair was delayed in AMPKα1$^{-/-}$ animals, from day 2 after injury (Fig.1E). First, in AMPKα1$^{-/-}$ mice, there was a significantly higher number of necrotic myofibers when compared with WT (+38% and +843% at day 2 and 4, $p<0.01$ and 0.05, respectively) (Fig.1E,F). A delay in the disappearance of damaged phagocyted myofibers was

also observed in AMPKα1$^{-/-}$ mice (+103% at day 4, p<0.01) (Fig.1E,F). Consequently, the number of newly-formed myofibers (appearing basophilic) was delayed (-56% and -10% at day 4 and 7, p<0.01, p<0.05, respectively) (Fig.1E,F). ~~At later time points, the size, or cross section area (CSA) of the new myofibers, which is an established indicator of the efficiency of muscle regeneration, was calculated. Fig.1E and G show that~~ 14 days after injury, the cross-section area (CSA) of the regenerating myofibers in AMPKα1$^{-/-}$ mice was smaller when compared with WT (55% decrease, p<0.001) (Fig.1E,G). The distribution of the myofiber CSA of AMPKα1$^{-/-}$ mice showed a shift to the left, exhibiting more small myofibers and fewer large myofibers (Fig.1E,G). Two months after injury (D56), a decrease of 37% in myofiber CSA was still observed in AMPKα1$^{-/-}$ muscle (p<0.05), indicating that muscle regeneration was impaired (Fig.1E,G). Due to a decrease in the myofiber size, a decrease in muscle mass was observed in AMPKα1$^{-/-}$ animals ~~(-11%, -14% and -28%, p<0.05, p<0.05 and p<0.001, for day 7, 14 and 21, respectively)~~ (Fig.1H). Several parameters related to myogenesis showed no difference between the two strains (data not shown). In WT and AMPKα1$^{-/-}$ muscles at day 0 and day 21, similar numbers were found of: i) myonuclei *per* fiber, suggesting that the fusion process was not altered by AMPKα1 deficiency; ii) Pax7^{+} satellite cells, suggesting no strong alteration in muscle cell homeostasis; iii) myofibers expressing succinate dehydrogenase (marker of oxidative metabolism) in WT and AMPKα1$^{-/-}$ muscles at day 0 and day 14, suggesting no alteration of myofiber metabolism during regeneration. Force measurement was not performed as previous studies showed that functional recovery after CTX injury is not achieved at 3 to 6 months in normal skeletal muscle despite normalized histology (Vignaud et al., 2005; Vignaud et al., 2006). Although one cannot exclude the contribution of AMPKα1 activity in several cell types (including myofibers) in the AMPKα1$^{-/-}$ total KO, particularly for the late time points, alteration of inflammation has previously been shown to directly impact muscle regeneration and myofiber size (Arnold et al., 2007; Perdiguero et al., 2011; Martinez et al., 2010).

Macrophagic AMPKα1 is required for proper skeletal muscle regeneration

Loss-of-function experiments were performed by crossing floxed AMPKα1 mice with the

myeloid specific LysM-CRE strain (Clausen et al., 1999). In the resulting LysM-CRE;AMPKα1$^{fl/fl}$ mice (named herein LysM-α1$^{-/-}$), AMPKα1 protein was undetectable in peritoneal macrophages (Suppl. Fig.2A). Percentage of deletion of AMPKα1 gene at the genomic level was null in tail (not shown), and increased to 73% in bone marrow (BM)-derived macrophages (BMDM) (compared with 49% in total BM), and to 84% in macrophages isolated from regenerating muscle (compared with 56% in muscle derived CD45^{+} cells), thus indicating the specificity of the deletion (Suppl. Fig.2B). AMPK levels were similar in resting muscle from AMPKα1$^{fl/fl}$ and LysM-α1$^{-/-}$ mice, indicating no leakage of LysM-Cre in myofibers (Suppl. Fig.2C).

Skeletal muscle regeneration in LysM-α1$^{-/-}$ mice showed a significant delay (Fig.2A-D). At day 7, an increase of necrotic/phagocytic myofibers was observed (+300%, $p<0.05$) (Fig.2A,B). At day 14, distribution of myofiber CSA showed a reduction in the size of regenerating myofibers ~~a shift to the left~~ in LysM-α1$^{-/-}$ when compared with WT muscle~~, indicative of a reduction in the size of regenerating myofibers~~ (Fig.2C)~~, although it was less pronounced than in total AMPKα1$^{-/-}$ muscle~~. Accordingly, mean CSA was decreased by 17% when compared with WT mice ($p<0.01$) (Fig.2A,D).

Rescue experiments included transplantation of AMPKα1$^{+/+}$;CX3CR1$^{GFP/+}$ and AMPKα1$^{-/-}$ CX3CR1$^{GFP/+}$ BM into total AMPKα1$^{-/-}$ recipients, hereafter indicated by BM^{WT}->KO and BM^{KO}->KO, respectively. Ten weeks after BM transplantation, recipient muscles were injured with CTX and analyzed 14 days later. Fig.2E shows infiltrating GFP^{pos} donor-derived cells in regenerating skeletal muscle of transplanted animals, indicating the efficiency of BM transplantation. Skeletal muscle regenerated in a much better way in the BM^{WT}->KO muscle when compared with BM^{KO}->KO (Fig.2F), as illustrated by a significant shift to the right of the distribution of the myofiber CSA (Fig.2G) and an increased mean CSA of regenerating myofibers (+49%, $p<0.001$) (Fig.2H). These results show that AMPKα1 is required for the regulation of macrophage functions during muscle regeneration.

AMPKα1$^{-/-}$ macrophages do not acquire M2 phenotypes *in vitro*

BMDM from WT and AMPKα1$^{-/-}$ animals were ~~analyzed for their ability to acquire polarized M1 and M2 phenotypes and relevant functions. BMDM were~~ polarized with cytokines to trigger various

inflammatory profiles. IFNγ, IL4 and IL10 treatments elicit pro-inflammatory (M1), alternative activation (M2a) and anti-inflammatory (M2c) states, respectively (Martinez et al., 2008). Twelve genes were analyzed by qRT-PCR (Suppl. Fig.3A). Results show that M1 polarization was achieved in these *in vitro* conditions: mRNAs of the M1 markers (*Tnf*, *il1b*, *ptgs2*, *Nos2*) were strongly expressed in M1 WT macrophages. High variations were observed among primary cultures for the expression of the M2 marker mRNAs (*Tgfb1*, *il10*, *il4ra*, *Vcam1*, *Chia*, *Arg1*, *Retnla*, *Chi3l3*), although a strong tendency towards an increase of some of these markers was observed in WT M2 *vs.* M1 macrophages, especially for M2a markers (*Chia*, *Arg1*, *Retnla*, *Chi3l3*) (Suppl.Fig.3A). As a whole, no significant difference of marker mRNA expression was observed between WT and AMPKα1$^{-/-}$ macrophages (Suppl. Fig.3A). As the regulation of inflammatory effectors is finely regulated at the post-transcriptional level (Lawrence and Natoli, 2011), expression of 7 markers of macrophage polarization~~proteins associated with the various inflammatory states of macrophages~~ was analyzed at the individual cell level by immunofluorescence. Fig.3A and Suppl. Fig.3B confirmed that the polarization was achieved in WT macrophages: a higher number of M1 macrophages expressed pro-inflammatory markers (CCL3, iNOS) in comparison with M2 macrophages. M2a and M2c macrophages higher expressed M2 markers (TGFβ1, CD206 and CD163)~~, when compared with M1 macrophages~~ (Fig.3A). Expression of COX-2 and Arginase-1 was not significantly ~~altered between the activation states~~changed (Fig.3A). AMPKα1$^{-/-}$ M1 macrophages showed no difference when compared with WT, except for ~~the number of macrophages expressing~~ iNOS expression, which was increased (+33%, $p<0.05$) (Fig.3A). Conversely, M2 macrophages (both M2a and M2c) derived from AMPKα1$^{-/-}$ mice exhibited altered activation profiles. A higher number of M1 markers-expressing cells was observed in AMPKα1$^{-/-}$ *vs.* WT M2 macrophages (+50 and +70% for CCL3 and iNOS, respectively, for M2c cells, $p<0.05$; +63% for iNOS for M2a cells, $p=0.055$). Moreover, the number of macrophages expressing M2 markers was decreased in both M2c (-33%, -21% and -56% for CD206, CD163 and TGFβ1, $p<0.01$, $p<0.05$, $p<0.01$, respectively) and M2a (-41% and -18% for CD206 and CD163, $p<0.001$ and $p<0.01$, respectively) macrophages (Fig.3A). Flow cytometry analysis showed that ~~, allowing the~~

~~evaluation of the intensity of the labeling. M~~mean Fluorescent Intensity of the M2 markers CD206 and Mgl1/CD301 was increased in WT M2a macrophages (+671% and +914% as compared with M1 cells, $p<0.05$) while a much weaker increase was observed in AMPKα1$^{-/-}$ macrophages (+441 and +449%, $p<0.05$) (Fig.3B). High oxygen consumption rate (OCR) has been shown to be associated with the M2 phenotype (Haschemi et al., 2012). As expected, M2a macrophages showed an increased basal and maximal OCR, as compared with M1 and M2c macrophages (+130 and +143% for basal and maximal OCR of M2a *vs.* M1 macrophages, $p<0.05$). This increase was not observed in AMPKα1$^{-/-}$ cells (Fig.3C). Moreover, activation of AMPK with AICAR induced a decrease of M1 (iNOS) and an increase of M2 (CD206) marker expression in WT macrophages while these changes were not observed in AMPKα1$^{-/-}$ macrophages (Fig.3D). Altogether, these results show that AMPKα1$^{-/-}$ macrophages were not able to fully adopt an M2 phenotype upon cytokine stimulation, and kept a pro-inflammatory profile.

We previously showed that M1 macrophages stimulate MPC proliferation while M2 macrophages promote their differentiation. This is of particular interest for myogenic cell fate during muscle regeneration where a sequential presence of M1, then M2 macrophages accompanies the regeneration process (Arnold et al., 2007; Saclier et al., 2013). Co-culture experiments were performed in which macrophage-conditioned medium was added to MPCs. ~~MPC proliferation was measured through ki67 labeling and myogenic differentiation was evaluated as the capacity of the cells to fuse together.~~ As expected, WT M1 macrophages stimulated MPC proliferation (+45%, $p<0.01$) (Fig.4A) while WT M2a and M2c macrophages promoted MPC fusion into myotubes (+63% and +57%, $p<0.05$ and $p<0.01$, respectively) (Fig.4B). ~~AMPKα1$^{-/-}$ M1 macrophages had the same effect as WT M1 macrophages on MPCs (Fig.4A,B). Conversely,~~ AMPKα1$^{-/-}$ M2 macrophages stimulated proliferation of MPCs (Fig.4A) while they were not able to sustain their fusion (Fig.4B). Moreover, conditioned medium from AICAR-treated WT macrophages stimulated MPC fusion, indicative of an M2 phenotype, while this increase was not observed in AMPKα1$^{-/-}$ macrophages (Fig.4C). These results confirmed that AMPKα1$^{-/-}$ macrophages failed to acquire an M2 phenotype.

AMPKα1$^{-/-}$ macrophages do not acquire M2 phenotype *in vivo*

Next, the capability of AMPKα1$^{-/-}$ macrophages to switch their phenotype was assessed *in vivo* during skeletal muscle regeneration. Flow cytometry analysis showed that the main CD45+ population was macrophages, from the first stages of muscle regeneration (72% at day 2, 75% at day 4), until the almost complete disappearance of CD45^{+} cells (35% at day 8~~). It is to note that neutrophils were transiently present (peak at day 2) and followed the same kinetics as LY6C^{hi}/CX3CR1-GFP^{lo} macrophages~~ (Fig.5A). CD45^{+} cells were extracted from regenerating WT and AMPKα1$^{-/-}$ muscle at different time points~~. Isolated CD45^{+} cells were then~~ and ~~tested for the expression of M1 and M2 markers~~analyzed by immunolabeling. In WT leukocytes, the number of cells expressing M1 markers (CCL3, iNOS) decreased with time (Fig.5B). Conversely, the number of cells positive for M2 markers (TGFβ1, CD206, CD163) increased during muscle regeneration, with the exception of Arginase 1 (Fig.5B). In AMPKα1$^{-/-}$ leukocytes, this kinetics was altered. The number of leukocytes expressing M1 markers was maintained while the number of leukocytes expressing M2 markers did not significantly increase during muscle regeneration (Fig.5B). These results show that intramuscular AMPKα1$^{-/-}$ macrophages did not acquire an M2 phenotype at the time of resolution of inflammation.

AMPKα1$^{+/+}$; CX3CR1$^{GFP/+}$ and AMPKα1$^{-/-}$; CX3CR1$^{GFP/+}$ mice were used to track neutrophils (Ly6C/G^{pos} CX3CR1/GFP^{neg}), M1 macrophages (Ly6C/G^{pos} CX3CR1/GFP^{lo}) and M2 macrophages (Ly6C/G^{neg} CX3CR1/GFP^{high}) during skeletal muscle repair~~. The GFP label, together with the LY6C/G(Gr1) label, allows for the identification of both circulating and infiltrating neutrophils (Ly6C/G^{pos} CX3CR1/GFP^{neg}), M1 macrophages (Ly6C/G^{pos} CX3CR1/GFP^{lo}) and M2 macrophages (Ly6C/G^{neg} CX3CR1/GFP^{high}) (Arnold et al., 2007; Geissmann et al., 2003)~~. This model has proven to be useful to track the early events of monocyte/macrophage subset infiltration into tissues and to follow their subsequent fate (Ginhoux et al., 2006; Zigmond et al., 2012; Rivollier et al., 2012). M2 macrophages expressed higher levels of the M2 marker CD206 at day 2 post-injury (Fig.6A). Homeostasis of circulating monocyte subsets in AMPKα1$^{-/-}$;CX3CR1$^{GFP/+}$ mice was not altered (data

not shown). Moreover, the number of infiltrating neutrophils and macrophages was similar in WT and AMPKα1$^{-/-}$ muscle 1 day after injury (Fig.6B), excluding a defect of leukodiapedesis in AMPKα1$^{-/-}$. At the time of resolution of inflammation, CX3CR1-GFP^{lo}Ly6C/G^{pos} cells convert into CX3CR1-GFP^{hi}Ly6C/G^{neg} cells (Arnold et al., 2007). The distribution of the two macrophage subsets was altered in AMPKα1$^{-/-}$ regenerating muscle, with a delay in the appearance of the M2 subset (Fig.6C). At day 1, a small number of M2 cells were present. In AMPKα1$^{-/-}$ muscle, M2 cells were already less numerous than in WT (-38.7%, p<0.05) (Fig.6C). From day 2, the switch from M1 to M2 occurred in WT. M2 cell number was still decreased in AMPKα1$^{-/-}$ muscle compared with WT (-14.0% at D2, P<0.05, -16.3% at D3, p=0.08) (Fig.6C). Accordingly, M2/M1 ratio was about 50% lower in AMPKα1$^{-/-}$ muscle for all time points (p<0.05) (Fig.6C). ~~To ascertain the specificity of AMPK deficiency, s~~Similar ~~experiments~~ results were obtained~~conducted~~ in LysM-α1$^{-/-}$ mice ~~and showed that at day 2 after injury,~~where the M2 subset was ~~also~~ reduced ~~in LysM-α1$^{-/-}$ muscle~~ as compared with the control (-11% at D2, p<0.05) (Fig.6D). Analysis was not carried on on later ~~on isolated CX3CR1-GFP$^{hi/lo}$ Ly6C/G$^{neg/pos}$ was performed only at early~~ time points since from day 4, the inflammatory phenotype of GFP^{pos} populations changes (Perdiguero et al., 2011). These results show that in the absence of AMPKα1, a part of M1 macrophages failed to switch to M2 at the time of resolution of inflammation.

AMPKα1$^{-/-}$ macrophages show a defect in phagocytosis ~~**associated with the impairment of the acquisition of the M2 phenotype**~~

~~We have previously shown that p~~Phagocytosis of necrotic/apoptotic MPCs by macrophages decreases their TNFα secretion and increase their TGFβ secretionindicating that phagocytosis of muscle debris participates to macrophage skewing (Arnold et al., 2007). Differentially activated macrophages exhibited a similar phagocytic activity of necrotic/apoptotic MPCs which is decreased in AMPKα1$^{-/-}$ macrophages (42% for M1 and 35% for M2a macrophages, p<0.05) (Fig.7A). ~~The phenotype of WT and AMPKα1$^{-/-}$ phagocyting M1 macrophages was then analyzed by immunofluorescence after incubation with apoptotic/necrotic MPCs.~~ As expected, in WT M1 macrophages, expression of M1 markers was decreased upon phagocytosis (by 36% and 34% for

iNOS and CCL3, $p<0.001$ and $p<0.01$, respectively) while that of M2 markers was increased (by 45%, 46% and 29% for TGFβ1, CD163 and CD206, $p<0.05$, $p<0.01$ and $p<0.01$, respectively) (Fig.7B). AMPKα1$^{-/-}$ macrophages did not present this phenotypic transition upon phagocytosis since the expression of neither of these markers was altered, except that of CD206, which was even decreased (Fig.7B). These results show that phagocytosis was impaired in AMPKα1$^{-/-}$ macrophages and that the phenotypic transition associated with phagocytosis could not properly operate in these cells.

AMPK activation can be triggered by upstream LKB1 and CaMKKβ kinases (Hawley et al., 2005; Woods et al., 2005). ~~We explored the potential involvement of these two pathways in the phenotype observed in AMPKα1$^{-/-}$ macrophages.~~ In mice deficient for LKB1 in the myeloid lineage (LysM-LKB1$^{-/-}$, Suppl. Fig.2D,E), no phenotypic difference was observed, as compared with the control. Muscle regeneration followed similar kinetics in LysM-LKB1$^{-/-}$ and control (LKB1$^{fl/fl}$) mice (Suppl. Fig.4A). The ratio between M1 and M2 macrophages at day 2 after injury was similar in both genotypes (Suppl. Fig.4B). These results suggest that LKB1 plays no or little role in AMPK activation in macrophages during muscle regeneration. To explore the role of CaMKKβ, we took advantage of the selective pharmacological CaMKK inhibitor STO-609 (Tokumitsu et al., 2002; Hawley et al., 2005; Woods et al., 2005), which leads to theinhibition of AMPK activation only it is activated by CaMKKβ (Hawley et al., 2010). We observed that WT M2 macrophages treated with STO-609 did not decrease the expression of the M1 marker iNOS and increased the expression of the M2 marker CD206 much weaker than untreated M2 macrophages (41 and 56% increase in STO-609 treated M2a and M2c *vs*. 68 and 70% in untreated macrophages, respectively) (Fig.7C). Moreover, phagocyting M1 macrophages treated with STO-609 did not decrease iNOS expression and did not increase CD206 expression, in contrast to untreated macrophages (Fig.7D). Finally, we analyzed the phosphorylation of AMPK with a specific antibody *in situ*, during skeletal muscle regeneration (Fig.7E). At day 2 post-injury, macrophages (F4/80^{+} cells) associated with phagocytosis of myofibers expressed p-AMPK while interstitial macrophages did not (Fig.7E). At day 7, almost all the myofibers were in a regenerating state, with remaining macrophages in the interstitium, which were not labeled for p-AMPK (Fig.7E). However,

rare isolated areas of single myofiber necrosis may still be observed. In these areas, macrophages carrying out phagocytosis were positive for p-AMPK. No labeling was observed in AMPKα1$^{-/-}$ muscle (Fig.7E). Altogether, these results suggest a link between phagocytosis of necrotic/apoptotic debris, CaMPKKβ and AMPK activation in the skewing of macrophages towards an M2 phenotype.

DISCUSSION

The results presented in this study show ~~a novel function for the energy-sensor AMPK. The~~ that absence of AMPKα1 in macrophages prevented their phenotypic transition during skeletal muscle regeneration and that AMPKα1$^{-/-}$ macrophages showed a defect in the acquisition of the M2 phenotypes, both *in vivo* and *in vitro*. Consequently, macrophage functions were altered and muscle regeneration was impaired.

AMPKα1 deficiency in macrophages prevented the acquisition of an M2 phenotype *in vitro*, as assessed by the lower expression of M2 markers and the higher expression of M1 markers upon IL4 and IL10 stimulation or AICAR treatment. ~~Inversely, stimulation of AMPK with AICAR triggered an M2 phenotype in macrophages.~~ Analyzing a battery of markers provide useful information on the *in vitro* activation of BMDM. First, the analysis of macrophage inflammatory state by RT-qPCR was not accurate with regard to the M2c phenotype. Only M1 state, and to some extent M2a, could be defined by RT-qPCR analysis. Secondly, the expression of markers at the mRNA level in the whole population and at the protein level in individual cells showed high discrepancies. These differences are likely due to the unexpected heterogeneity of the macrophage populations. Our results show that~~Indeed, the immunolabeling experiments showed that,~~ although stimulated by a unique cytokine, the macrophage populations remained heterogeneous: all the tested markers were expressed by both M1, M2a and M2c macrophages by at least 15% or 30% of the cells. Finally, COX-2 (*ptgs2*) and Arginase 1 (*Arg1*), which are considered as "canonical" markers to define M1 and M2 activation, respectively, were not useful to discriminate mouse macrophage activation states in our setting ~~*in vitro*~~. ~~Moreover, the expression of these two markers did not vary in muscle-derived~~

~~macrophages during regeneration.~~ These results indicate that a series of markers should be examined at the cellular level to properly assess macrophage inflammatory state.

Several functions were found altered in AMPKα1$^{-/-}$ macrophages. ~~Recent studies reported that a~~A metabolic switch is associated with the distinct functions of M1 and M2 macrophages (Vats et al., 2006; Rodriguez-Prados et al., 2010; Haschemi et al., 2012). M2a AMPKα1$^{-/-}$ macrophages did not display ~~such the~~an increase of oxidative phosphorylation observed in WT M2a macrophages, confirming that induction of mitochondrial fatty acid oxidation is ~~a critical factor~~ related to the M2 phenotype. Similarly, AMPKβ1 deficiency in macrophages results in reduced rates of fatty acid oxidation and altered M1/M2 polarization (Galic et al., 2011). Moreover, *in vitro* functional analysis showed that AMPKα1$^{-/-}$ macrophages prone to M2 polarization were not able to sustain myogenesis. They stimulated MPC proliferation and inhibited MPC fusion just as WT M1 macrophages did, indicating that they did not acquire an M2 phenotype. During muscle regeneration, p M1 macrophages firt stimulate MPC proliferation, then M2 macrophages stimulate terminal myogenesis (Arnold et al., 2007; Saclier et al., 2013). The defect of M2 AMPKα1$^{-/-}$ macrophages to sustain *in vitro* myogenesis explains the impairment of regeneration observed in AMPKα1$^{-/-}$ and LysM-α1$^{-/-}$ muscles. Inversely, activating AMPK with AICAR in macrophages promoted myogenesis through their skewing into M2 cells. Therefore, beside its direct effects on myofiber energy metabolism (Narkar et al., 2011), AMPK may indirectly act on myogenesiss through the properties of macrophages during muscle regeneration.

In vivo investigations confirmed the *in vitro* results. ~~Analysis of the macrophage subsets in the CX3CR1$^{GFP/+}$ mouse showed that i~~In AMPKα1$^{-/-}$ and LysM-α1$^{-/-}$ muscle, the number of CX3CR1-GFP^{hi}Ly6C/G^{neg} (M2) cells was decreased to the benefit of CX3CR1-GFP^{lo}Ly6C/G^{pos} (M1) cells, indicating a defect in macrophage skewing ~~during skeletal muscle regeneration~~. Moreover, ~~analysis of inflammatory markers on isolated CD45^{+} cells showed that in WT muscle-derived leukocytes,~~ the the kinetics of expression of M1 and M2 markers by isolated CD45^{+} leukocytes was totally impaired ~~expression of M1 markers decreased with time while that of M2 markers increased. This was not~~

~~observed~~ in AMPKα1$^{-/-}$ muscle, meaning that AMPKα1$^{-/-}$ macrophages were not capable of acquiring an M2 phenotype during muscle regeneration.

Consequently, impairment and delay in muscle regeneration was observed in LysM-α1$^{-/-}$ muscle while a benefit was observed after WT BM transplantation into AMPKα1$^{-/-}$ recipients. The benefit did not fully correct the delay of regeneration that was observed in total AMPKα1$^{-/-}$ mice. Moreover, regeneration defects observed in total AMPKα1$^{-/-}$ were more pronounced than in LysM-α1$^{-/-}$ muscle. This indicates that AMPKα1 expressed in other cell types likely contributes to muscle regeneration. Although we found no difference in several myogenic parameters, ~~the number of myonuclei, satellite cells, repartition of glycolytic/oxidative myofibers~~ between WT and AMPKα1$^{-/-}$ muscle~~ after completion of the regeneration process~~, one cannot exclude a role of AMPKα1, particularly in the late phases of muscle regeneration, in non-myeloid cells, including myofibers. Indeed, it has been involved in the control of muscle cell and myofiber size (Lantier et al., 2010; Mounier et al., 2009). Other cell types including eosinophils and fibro-adipogenic precursors have been shown to play crucial roles for a proper muscle regeneration (Joe et al., 2010; Uezumi et al., 2010; Heredia et al., 2013). Finally, ~~Recent studies investigating the role of AMPK in inflammation focused on the role of AMPK in a unique pro-inflammatory (*e.g.* LPS stimulation) context, in which blocking AMPK increases the pro-inflammatory status of macrophages. Ss~~several signaling pathways ~~were~~ have been implicated in the modulation of LPS-induced M1 macrophages by AMPK, including MAPKs, PI3K/Akt and NFκB (Jeong et al., 2009; Peairs et al., 2009; Sag et al., 2008; Yi et al., 2011; Giri et al., 2004). During skeletal muscle regeneration, inhibition of Cebpβ function is associated with increased M1 markers upon LPS stimulation *in vitro* and leads to defects in muscle fiber regeneration *in vivo* (Ruffell et al., 2009). Restriction of p38 MAPK activation by MKP-1 (MAPK phosphatase-1) was shown to control macrophage phenotypic transition and muscle recovery (Perdiguero et al., 2011). It is likely that several signaling pathways act together to operate the tight regulation of macrophage skewing at the time of resolution of inflammation.

The mechanisms by which macrophages operate the transition from M1 to M2 phenotype are poorly characterized. Phagocytosis of tissue debris has been involved since anti-inflammatory effectors are increased in phagocyting macrophages while pro-inflammatory compounds are down-regulated (Fadok et al., 1998; Freire-de-Lima et al., 2006; Johann et al., 2006). A few reports investigated the intracellular signaling downstream of dead cell recognition: inhibition of IL12 synthesis is regulated by GC binding protein (GC-BP) (Kim et al., 2004) while production of IL10 is regulated by Pbx1 and Prep-1 transcription factors activated through the p38 signaling pathway (Chung et al., 2007). We previously showed that macrophages that have phagocyted apoptotic/necrotic MPCs skew their phenotype towards an M2 profile (Arnold et al., 2007). More recently, it has been shown that fibro-adipogenic precursors are also capable of phagocytosis during skeletal muscle regeneration, emphasizing the role of phagocytosis in this process (Heredia et al., 2013). Here, we observed that AMPKα1 deficiency led to a strong decrease in macrophage phagocytic activity. Accordingly, phosphorylated-AMPK was found associated only with macrophages operating phagocytosis of necrotic myofibers in regenerating muscle (Fig.7). Our result are in line with the increased phagocytic activity (of *E.Coli*) of macrophages upon AICAR treatment (Bae et al., 2011). Moreover, the defect of phagocytosis of AMPKα1-/- macrophages is associated with their inability to operate the phenotypic transition from M1 to M2, explaining the alteration of regeneration observed in AMPKα1$^{-/-}$ and LysM-α1$^{-/-}$ muscles, the persistence of necrotic/phagocytic myofibers (Fig.1) and the increased number of neutrophils at day 2 in AMPKα1$^{-/-}$ muscle (Fig.5). Interestingly, apoptotic cell recognition induces both an acute and sustained calcium flux within phagocytes and the molecules required for calcium flux are essential for engulfment (Gronski et al., 2009). CaMKKα inhibition blocks M2 type macrophage activation and promotes M1 activation (Guest et al., 2008). Moreover, CaMKKs are capable of activating AMPK (Hurley et al., 2005; Hawley et al., 2005; Woods et al., 2005). We showed here that inhibition of CaMKKβ with STO-609 prevented the acquisition of the M2 phenotype by both upon cytokine stimulation and pro-inflammatory macrophages phagocyting necrotic/apoptotic MPCs. Further studies are required to decipher to

which extent phagocytosis causes the activation of the CaMMKβ/AMPK axis, or whether CaMMKβ/AMPK is required for phagocytosis. Altogether, our results suggest a link between the CaMKKβ/AMPK axis and phagocytosis, phagocytosis being one of the most efficient mechanisms regulating the transition of macrophage towards an M2 phenotype at the time of resolution of inflammation.

EXPERIMENTAL PROCEDURES

Complete experimental procedures are provided in supplementary information.

Mice and mouse experiments. Adult male animals from AMPKα1$^{-/-}$, AMPKα1$^{fl/fl}$, LysM-CRE$^{+/-}$:AMPKα1$^{fl/fl}$, CX3CR1$^{GFP/+}$; CXRCR1$^{GFP/+}$:AMPKα1$^{-/-}$, LysM-CRE$^{+/-}$:LKB1$^{fl/fl}$, LKB1$^{fl/fl}$ mouse strains were used. Muscle injury was caused by intramuscular injection of CTX in the TA muscle and BM transplantation was performed as previously described (Perdiguero et al., 2011).

Isolation of leukocytes and macrophages from muscle. The muscles were minced and digested with collagenase B 0.2%. CD45^{+} cells were isolated using magnetic sorting (Miltenyi Biotec) and labeled with APC-conjugated anti-Gr1 (Ly6C/G) or anti-F4/80 (ebioscience) antibodies. Cells were analyzed using a flow cytometer (FC-500; Beckman Coulter) or a FACS Canto II (BD biosciences) using Diva and FlowJo software. In some experiments, CD45+ cells were cytospined (Cellspin I, Tharmac) on starfrost slides and immunostained (see below). In some experiments, macrophage subsets were sorted using a FACSAria III cell sorter (BD Biosciences).

Macrophage cell culture. Macrophages were obtained from BM precursor cells. Briefly, total BM was obtained from mice by flushing femurs and tibiae BM with DMEM. Cells were cultured in DMEM medium containing conditioned medium of L929 cell line (enriched in CSF-1) for 7 days. Macrophages were activated with cytokines to obtain various activation states: IFNγ (50 ng/ml), IL4 (10 ng/ml), IL10 (10 ng/ml) to obtain M1, M2a and M2c macrophages, respectively in DMEM containing 10% FBS medium for 3 days. In some experiments, macrophages were incubated with 1 mM AICAR (Tocris) for 4 h or with 5 µM STO-609 (Tocris) or DMSO for 3 days in DMEM containing

10% FBS medium. After washing steps, DMEM serum-free medium was added for 24 h, recovered and centrifugated to obtain macrophage-conditioned medium, or cells were directly used for various analyses.

MPC culture. Murine MPCs were obtained from TA muscle and cultured using standard conditions in DMEM/ F12 (Gibco Life Technologies) containing 20% Fetal Bovine serum (FBS) and 2% G/Ultroser (Pall Inc). For proliferation studies, MPCs were seeded at 10000 cell/cm^2 on matrigel (1/10) and incubated for 1 day with MP-conditioned medium + 2.5% FBS. Cells were then incubated with anti-ki67 antibodies (15580 Abcam). For differentiation studies, MPCs were seeded at 30000 cell/cm^2 on matrigel (1/10) and incubated for 3 days with macrophage-conditioned medium containing 2% horse serum. Cells were then incubated with anti-desmin antibodies (32362 Abcam).

***In vitro* immunolabelings.** Macrophages were labeled with primary antibodies against the following proteins: CCL3 (sc-1383 Santa-cruz), COX2 (ab2372 Abcam), iNOS (ab3523 Abcam), CD206 (sc-58987 Santa Cruz), CD163 (sc-33560 Santa-cruz), TGFβ1 (ab64715 Abcam), Arginase 1 (sc-18355 Santa Cruz), revealed with a cy3-conjugated secondary antibody (Jackson Immunoresearch Inc).

Phagocytosis assay. MPCs were labeled with PKH67 (Sigma Aldrich), then treated with staurosporin at 5 µM for 4 h to induce apoptosis. Polarized macrophages were incubated with apoptotic MPCs at a 1:5 ratio for 30 min at 4°C or 6 h at 37°C. After 5-6 PBS washings, cultures were trypsinized, cells were labeled with F4/80-PeCy7 antibody (ebiosciences) and analyzed by flow cytometry (FC-500; Beckman Coulter). The double positive cells ($F4/80^{pos}PKH67^{pos}$) cells were phagocytic macrophages while the $F4/80^{pos}PKH67^{neg}$ cells were non-phagocytic macrophages. To exclude macrophages that have bound but not ingested apoptotic cells, the percentage of double positive cells observed at 4°C (binding occurs but not endocytosis) was substracted from the value observed at 37°C. In some experiments, 5 µM STO-609 (or DMSO) was added at the time of phagocytosis.

Statistical analyses. All experiments were performed using at least three independent primary cultures or at least 5 animals for *in vivo* analyses. Isolation of macrophages from regenerating muscle

required for each experiment, 3, 2, 5 mice at 2, 4 and 7 days after injury, respectively. Depending of the experiments, the Student's t-test or two-way ANOVA test was performed and Bonferroni post-tests were applied. $P<0.05$ was considered significant.

REFERENCES

Arnold, L., Henry, A., Poron, F., Baba-Amer, Y., van Rooijen, N., Plonquet, A., Gherardi, R.K., and Chazaud, B. (2007). Inflammatory monocytes recruited after skeletal muscle injury switch into antiinflammatory macrophages to support myogenesis. J. Exp. Med. *204*, 1071-1081.

Bae, H.B., Zmijewski, J.W., Deshane, J.S., Tadie, J.M., Chaplin, D.D., Takashima, S., and Abraham, E. (2011). AMP-activated protein kinase enhances the phagocytic ability of macrophages and neutrophils. FASEB J *25*, 4358-4368.

Chung, E.Y., Liu, J., Homma, Y., Zhang, Y., Brendolan, A., Saggese, M., Han, J., Silverstein, R., Selleri, L., and Ma, X. (2007). Interleukin-10 expression in macrophages during phagocytosis of apoptotic cells is mediated by homeodomain proteins Pbx1 and Prep-1. Immunity. *27*, 952-964.

Clausen, B.E., Burkhardt, C., Reith, W., Renkawitz, R., and Forster, I. (1999). Conditional gene targeting in macrophages and granulocytes using LysMcre mice. Transgenic Res. *8*, 265-277.

Fadok, V.A., Bratton, D.L., Konowal, A., Freed, P.W., Westcott, J.Y., and Henson, P.M. (1998). Macrophages that have ingested apoptotic cells in vitro inhibit proinflammatory cytokine production through autocrine/paracrine mechanisms involving TGF-beta, PGE2, and PAF. J. Clin. Invest. *101*, 890-898.

Freire-de-Lima, C.G., Xiao, Y.Q., Gardai, S.J., Bratton, D.L., Schiemann, W.P., and Henson, P.M. (2006). Apoptotic cells, through transforming growth factor-beta, coordinately induce anti-inflammatory and suppress pro-inflammatory eicosanoid and NO synthesis in murine macrophages. J. Biol. Chem. *281*, 38376-38384.

Galic, S., Fullerton, M.D., Schertzer, J.D., Sikkema, S., Marcinko, K., Walkley, C.R., Izon, D., Honeyman, J., Chen, Z.P., van Denderen, B.J., et al (2011). Hematopoietic AMPK beta1 reduces mouse adipose tissue macrophage inflammation and insulin resistance in obesity. J Clin Invest. *121*, 4903-4915.

Geissmann, F., Jung, S., and Littman, D.R. (2003). Blood monocytes consist of two principal subsets with distinct migratory properties. Immunity *19*, 71-82.

Ginhoux, F., Tacke, F., Angeli, V., Bogunovic, M., Loubeau, M., Dai, X.M., Stanley, E.R., Randolph, G.J., and Merad, M. (2006). Langerhans cells arise from monocytes in vivo. Nat. Immunol. *7*, 265-273.

Giri, S., Nath, N., Smith, B., Viollet, B., Singh, A.K., and Singh, I. (2004). 5-aminoimidazole-4-carboxamide-1-beta-4-ribofuranoside inhibits proinflammatory response in glial cells: a possible role of AMP-activated protein kinase. J Neurosci. *24*, 479-487.

Gronski, M.A., Kinchen, J.M., Juncadella, I.J., Franc, N.C., and Ravichandran, K.S. (2009). An essential role for calcium flux in phagocytes for apoptotic cell engulfment and the anti-inflammatory response. Cell Death. Differ. *16*, 1323-1331.

Guest, C.B., Deszo, E.L., Hartman, M.E., York, J.M., Kelley, K.W., and Freund, G.G. (2008). Ca2+/calmodulin-dependent kinase kinase alpha is expressed by monocytic cells and regulates the activation profile. PLoS One. *3*, e1606.

Hardie, D.G. (2011). AMP-activated protein kinase: an energy sensor that regulates all aspects of cell function. Genes Dev. *25*, 1895-1908.

Haschemi, A., Kosma, P., Gille, L., Evans, C.R., Burant, C.F., Starkl, P., Knapp, B., Haas, R., Schmid, J.A., Jandl, C., et al (2012). The sedoheptulose kinase CARKL directs macrophage polarization through control of glucose metabolism. Cell Metab *15*, 813-826.

Hawley, S.A., Pan, D.A., Mustard, K.J., Ross, L., Bain, J., Edelman, A.M., Frenguelli, B.G., and Hardie, D.G. (2005). Calmodulin-dependent protein kinase kinase-beta is an alternative upstream kinase for AMP-activated protein kinase. Cell Metab *2*, 9-19.

Hawley, S.A., Ross, F.A., Chevtzoff, C., Green, K.A., Evans, A., Fogarty, S., Towler, M.C., Brown, L.J., Ogunbayo, O.A., Evans, A.M., et al (2010). Use of cells expressing gamma subunit variants to identify diverse mechanisms of AMPK activation. Cell Metab. *11*, 554-565.

Heredia, J.E., Mukundan, L., Chen, F.M., Mueller, A.A., Deo, R.C., Locksley, R.M., Rando, T.A., and Chawla, A. (2013). Type 2 innate signals stimulate fibro/adipogenic progenitors to facilitate muscle regeneration. Cell *153*, 376-388.

Hurley, R.L., Anderson, K.A., Franzone, J.M., Kemp, B.E., Means, A.R., and Witters, L.A. (2005). The Ca2+/calmodulin-dependent protein kinase kinases are AMP-activated protein kinase kinases. J Biol Chem *280*, 29060-29066.

Jeong, H.W., Hsu, K.C., Lee, J.W., Ham, M., Huh, J.Y., Shin, H.J., Kim, W.S., and Kim, J.B. (2009). Berberine suppresses proinflammatory responses through AMPK activation in macrophages. Am. J. Physiol. Endocrinol. Metab. *296*, E955-E964.

Joe, A.W., Yi, L., Natarajan, A., Le Grand, F., So, L., Wang, J., Rudnicki, M.A., and Rossi, F.M. (2010). Muscle injury activates resident fibro/adipogenic progenitors that facilitate myogenesis. Nat. Cell Biol. *12*, 153-163.

Johann, A.M., von Knethen, A., Lindemann, D., and Brune, B. (2006). Recognition of apoptotic cells by macrophages activates the peroxisome proliferator-activated receptor-gamma and attenuates the oxidative burst. Cell Death Differ. *13*, 1533-1540.

Kim, S., Elkon, K.B., and Ma, X. (2004). Transcriptional suppression of interleukin-12 gene expression following phagocytosis of apoptotic cells. Immunity. *21*, 643-653.

Lantier, L., Mounier, R., Leclerc, J., Pende, M., Foretz, M., and Viollet, B. (2010). Coordinated maintenance of muscle cell size control by AMP-activated protein kinase. FASEB J *24*, 3555-3561.

Lawrence, T. and Fong, C. (2010). The resolution of inflammation: anti-inflammatory roles for NF-kappaB. Int. J Biochem. Cell Biol. *42*, 519-523.

Lawrence, T. and Natoli, G. (2011). Transcriptional regulation of macrophage polarization: enabling diversity with identity. Nat. Rev. Immunol. *11*, 750-761.

Martinez, C.O., McHale, M.J., Wells, J.T., Ochoa, O., Michalek, J.E., McManus, L.M., and Shireman, P.K. (2010). Regulation of skeletal muscle regeneration by CCR2-activating chemokines is directly related to macrophage recruitment. Am J Physiol Regul Integr Comp Physiol *299*, R832-R842.

Martinez, F.O., Sica, A., Mantovani, A., and Locati, M. (2008). Macrophage activation and polarization. Front Biosci *13*, 453-461.

Mosser, D.M. and Edwards, J.P. (2008). Exploring the full spectrum of macrophage activation. Nat. Rev. Immunol. *8*, 958-969.

Mounier, R., Lantier, L., Leclerc, J., Sotiropoulos, A., Pende, M., Daegelen, D., Sakamoto, K., Foretz, M., and Viollet, B. (2009). Important role for AMPK{alpha}1 in limiting skeletal muscle cell hypertrophy. FASEB J. *23*, 2264-2273.

Narkar, V.A., Fan, W., Downes, M., Yu, R.T., Jonker, J.W., Alaynick, W.A., Banayo, E., Karunasiri, M.S., Lorca, S., and Evans, R.M. (2011). Exercise and PGC-1alpha-independent synchronization of type I muscle metabolism and vasculature by ERRgamma. Cell Metab *13*, 283-293.

Peairs, A., Radjavi, A., Davis, S., Li, L., Ahmed, A., Giri, S., and Reilly, C.M. (2009). Activation of AMPK inhibits inflammation in MRL/lpr mouse mesangial cells. Clin Exp Immunol *156*, 542-551.

Perdiguero, E., Sousa-Victor, P., Ruiz-Bonilla, V., Jardi, M., Caelles, C., Serrano, A.L., and Munoz-Canoves, P. (2011). p38/MKP-1-regulated AKT coordinates macrophage transitions and resolution of inflammation during tissue repair. J. Cell Biol. *195*, 307-322.

Rivollier, A., He, J., Kole, A., Valatas, V., and Kelsall, B.L. (2012). Inflammation switches the differentiation program of Ly6Chi monocytes from antiinflammatory macrophages to inflammatory dendritic cells in the colon. J Exp Med. *1*, 139-155.

Rodriguez-Prados, J.C., Traves, P.G., Cuenca, J., Rico, D., Aragones, J., Martin-Sanz, P., Cascante, M., and Bosca, L. (2010). Substrate fate in activated macrophages: a comparison between innate, classic, and alternative activation. J Immunol. *185*, 605-614.

Ruffell, D., Mourkioti, F., Gambardella, A., Kirstetter, P., Lopez, R.G., Rosenthal, N., and Nerlov, C. (2009). A CREB-C/EBPbeta cascade induces M2 macrophage-specific gene expression and promotes muscle injury repair. Proc. Natl. Acad. Sci. USA *106*, 17475-17480.

Saclier, M., Yacoub-Youssef, H., Mackey, A.L., Arnold, L., Ardjoune, H., Magnan, M., Sailhan, F., Chelly, J., Pavlath, G.K., Mounier, R., et al (2013). Differentially activated macrophages orchestrate myogenic precursor cell fate during human skeletal muscle regeneration. Stem Cells *31*, 384-396.

Sag, D., Carling, D., Stout, R.D., and Suttles, J. (2008). Adenosine 5'-monophosphate-activated protein kinase promotes macrophage polarization to an anti-inflammatory functional phenotype. J. Immunol. *181*, 8633-8641.

Sun, D., Martinez, C.O., Ochoa, O., Ruiz-Willhite, L., Bonilla, J.R., Centonze, V.E., Waite, L.L., Michalek, J.E., McManus, L.M., and Shireman, P.K. (2009). Bone marrow-derived cell regulation of skeletal muscle regeneration. FASEB J. *23*, 382-395.

Tokumitsu, H., Inuzuka, H., Ishikawa, Y., Ikeda, M., Saji, I., and Kobayashi, R. (2002). STO-609, a specific inhibitor of the Ca(2+)/calmodulin-dependent protein kinase kinase. J Biol. Chem. *277*, 15813-15818.

Uezumi, A., Fukada, S., Yamamoto, N., Takeda, S., and Tsuchida, K. (2010). Mesenchymal progenitors distinct from satellite cells contribute to ectopic fat cell formation in skeletal muscle. Nat. Cell Biol. *12*, 143-152.

Vats, D., Mukundan, L., Odegaard, J.I., Zhang, L., Smith, K.L., Morel, C.R., Wagner, R.A., Greaves, D.R., Murray, P.J., and Chawla, A. (2006). Oxidative metabolism and PGC-1beta attenuate macrophage-mediated inflammation. Cell Metab *4*, 13-24.

Vignaud, A., Caruelle, J.P., Martelly, I., and Ferry, A. (2006). Differential effects of post-natal development, animal strain and long term recovery on the restoration of neuromuscular function after neuromyotoxic injury in rat. Comp Biochem. Physiol C. Toxicol. Pharmacol. *143*, 1-8.

Vignaud, A., Hourde, C., Torres, S., Caruelle, J.P., Martelly, I., Keller, A., and Ferry, A. (2005). Functional, cellular and molecular aspects of skeletal muscle recovery after injury induced by snake venom from Notechis scutatus scutatus. Toxicon *45*, 789-801.

Woods, A., Dickerson, K., Heath, R., Hong, S.P., Momcilovic, M., Johnstone, S.R., Carlson, M., and Carling, D. (2005). Ca2+/calmodulin-dependent protein kinase kinase-beta acts upstream of AMP-activated protein kinase in mammalian cells. Cell Metab *2*, 21-33.

Xing, J., Wang, Q., Coughlan, K., Viollet, B., Moriasi, C., and Zou, M.H. (2013). Inhibition of AMP-Activated Protein Kinase Accentuates Lipopolysaccharide-Induced Lung Endothelial Barrier Dysfunction and Lung Injury in Vivo. Am J Pathol *182*, 1021-1030.

Yi, C.O., Jeon, B.T., Shin, H.J., Jeong, E.A., Chang, K.C., Lee, J.E., Lee, D.H., Kim, H.J., Kang, S.S., Cho, G.J., et al (2011). Resveratrol activates AMPK and suppresses LPS-induced NF-kappaB-dependent COX-2 activation in RAW 264.7 macrophage cells. Anat Cell Biol *44*, 194-203.

Zhao, X., Zmijewski, J.W., Lorne, E., Liu, G., Park, Y.J., Tsuruta, Y., and Abraham, E. (2008). Activation of AMPK attenuates neutrophil proinflammatory activity and decreases the severity of acute lung injury. Am J Physiol Lung Cell Mol Physiol *295*, L497-L504.

Zigmond, E., Varol, C., Farache, J., Elmaliah, E., Satpathy, A.T., Friedlander, G., Mack, M., Shpigel, N., Boneca, I.G., Murphy, K.M., et al (2012). Ly6C(hi) Monocytes in the Inflamed Colon Give Rise to Proinflammatory Effector Cells and Migratory Antigen-Presenting Cells. Immunity. *37*, 1076-1090.

ACKNOWLEDGEMENTS

This work was funded by grants from Institut Cochin (PIC), the European Commission integrated project (LSHM-CT-2004-005272), the Framework Programme FP7 under grant agreement n° [241440] Endostem, Association Française contre les Myopathies, Association Française pour la Lutte contre le Dopage, and Société Française de Myologie. We thank D.G. Hardie (Dundee University, Scotland, UK) for providing anti AMPKα1 antibodies and R. DePinho (University of Texas, USA) for providing the $LKB1^{fl/fl}$ mice.

Figure Legends

Figure 1 – Effects of AMPKα1 loss on skeletal muscle regeneration. WT (white bars) and AMPKα1$^{-/-}$ (black bars) TA muscle was injured with CTX and analyzed at several days (D in X axes) after injury. **(A)** AMPKα1 activity measured in whole WT muscle. **(B)** Percentage of GFP^{pos} cells, *i.e*. macrophages from WT regenerating CX3CR1$^{GFP/+}$ mouse muscle. **(C)** AMPKα1 activity measured in F4/80^{+} macrophages isolated from WT regenerating mouse muscle. Each symbol represents one independent experiment. **(D)** AMPKα2 activity measured in whole muscle. **(E)** HE staining of regenerating muscle. Crosses (x) indicate necrotic myofibers, asterisks (*) show phagocyted myofibers, arrows indicate basophilic myofibers. **(F)** Quantification of regeneration assessed by the percentage of necrotic, phagocyted, regenerating (basophilic) and regenerating (centrally nucleated) myofibers expressed in percentage of the total number or myofibers. **(G)** Distribution of myofiber CSA at day 14 post-injury (left) and mean CSA (right). **(H)** Specific mass of TA muscle. Results are means ± s.e.m. from at least 5 animals. *p<0.05, **p<0.01, ***p<0.001 AMPKα1$^{-/-}$ *vs.* WT. $^{\#}$p<0.05, $^{\#\#}$p<0.01, $^{\#\#\#}$p<0.001 *vs.* D0 or D2. Bar = 50 µm.

Figure 2 – Effects of loss-of-function and rescue of macrophagic AMPKα1 on skeletal muscle regeneration. (A-D) In loss-of-function experiments, LysM-α1$^{-/-}$ and AMPKα1$^{fl/fl}$ (as a control) TA muscles were injured with CTX and analyzed 7 (D7) and 14 (D14) days after injury. **(A)** HE staining of regenerating muscle. **(B)** Quantification of necrotic and phagocyted myofibers expressed in percentage of the total number of myofibers. **(C)** Distribution and **(D)** mean of myofiber CSA. **(E-H)** In rescue experiments, BM transplantation of AMPKα1$^{-/-}$ mice was performed with WT BM (BM^{WT}->KO) or with AMPKα1$^{-/-}$ BM (BM^{KO}->KO) as a control. Ten weeks later, TA muscle was injured with CTX and analyzed 14 days later. **(E)** Presence of GFP^{+} (green) macrophages from donor (CX3CR1$^{GFP/+}$ mouse) in recipient regenerating muscle. Laminin staining in red, nuclei in blue. **(F)** HE staining of regenerating muscle. **(G)** Distribution and **(H)** mean of myofiber CSA. Results are means ± s.e.m. from at least 5 animals. *p<0.05, **p<0.01, ***p<0.001 *vs.* WT. Bar in A and F= 50 µm. Bar in E = 100 µm.

Figure 3 – Effects of AMPKα1 loss on macrophage inflammatory phenotype after *in vitro* polarization. WT and AMPKα1$^{-/-}$ BMDM were activated into M1, M2c and M2a macrophages with IFNγ, IL10 and IL4 treatment, respectively, for 3 days. **(A)** Cells were tested for the expression of a series of M1 and M2 markers by immunofluorescence. Results are expressed as percentage of positive cells. **(B)** M2 markers (CD206, Mgl1/CD301) were analyzed by flow cytometry. Left: evaluation of specific Mean Fluorescence Intensity . Right: representative histograms of M2a macrophages. **(C)** Measurement of OCR in basal conditions (Basal) or after stimulation of WT and AMPKα1$^{-/-}$ (KO) macrophages with CCCP (Max). **(D)** Expression of iNOS and CD206 after stimulation of macrophages with AICAR. Results are means ± s.e.m. of at least 3 independent experiments. *p<0.05, **p<0.01, ***p<0.001 AMPKα1$^{-/-}$ *vs.* WT. $^{\#}$p<0.05, $^{\#\#}$p<0.01 *vs.* M1. £ p<0.05 *vs*. non treated cells (NT). Bar = 20 µm.

Figure 4 – Effects of AMPKα1 loss on macrophage functions after *in vitro* polarization. WT and AMPKα1$^{-/-}$ BMDM were polarized as in Fig.3 **(A,B)** or were treated with AICAR **(C)** and conditioned medium was added to MPCs. **(A)** MPC proliferation was measured as the percentage of ki67 positive cells (red: ki67, blue: Hoechst). **(B,C)** MPC fusion index was calculated after desmin labeling (red: desmin, blue: Hoechst). Results are means ± s.e.m. of at least 3 independent experiments. *p<0.05,**p<0.01 AMPKα1$^{-/-}$ *vs.* WT. $^{\#}$p<0.05, $^{\#\#}$p<0.01 $^{\#\#\#}$p<0.001 *vs.* M1. $^{\$}$p<0.05, $^{\$\$}$p<0.01 *vs.* None. $^{£}$p<0.05, $^{££}$p<0.01 *vs*. untreated cells (NT). Bar = 20 µm.

Figure 5 – Effects of AMPKα1 loss on *in vivo* macrophage inflammatory phenotype during muscle regeneration. (A) The number of CD45+ cell populations was evaluated by flow cytometry analysis during muscle regeneration and expressed *per* mg of muscle. **(B)** WT (white circles) and AMPKα1$^{-/-}$ (black circles) TA muscle was injured with CTX and CD45^{+} cells were extracted at several days (D in X axes) after injury, cytospined and tested for the expression of M1 and M2 markers by immunofluorescence. Results are expressed as percentage of positive cells and are means ± s.e.m. of at least 3 independent experiments. *p<0.05 AMPKα1$^{-/-}$ *vs.* WT. $^{\#}$p<0.05, $^{\#\#}$p<0.01 *vs.* D2. Bar = 20 µm.

Figure 6 – Effects of AMPKα1 loss on the switch of macrophage inflammatory phenotype during muscle regeneration. TA muscle was injured with CTX, and was analyzed for cell population repartition by flow cytometry after extraction of $CD45^+$ cells. **(A)** In WT ($AMPK\alpha1^{+/+}$;$CX3CR1^{GFP/+}$) and $AMPK\alpha1^{-/-}$ ($AMPK\alpha1^{-/-}$;$CX3CR1^{GFP/+}$) muscle, 3 populations can be separated: $CX3CR1/GFP^{neg}$ $Ly6C/G^{hi}$ (neutrophils, N), $CX3CR1/GFP^{lo}$ $Ly6C/G^{hi}$ (M1) and $CX3CR1/GFP^{hi}$ $Ly6C/G^{neg}$ (M2) macrophage (example of a dot plot at day 2 after injury). Below, histograms of CD206 immunolabeling show a higher expression by $Ly6C^{lo}$ macrophages, confirming their M2 phenotype. **(B)** The number of macrophages ($CXRCR1/GFP^{pos}$ cells) and neutrophils was evaluated *per* mg of muscle 1 day after injury. **(C)** M2 macrophage number was expressed as a percentage of total macrophages at day 1, 2 and 3 after injury. The M2/M1 ratio is given in the right panel. **(D)** Similar analyses of macrophage subsets were performed in LysM-$\alpha1^{-/-}$ (vs. $AMPK1^{fl/fl}$) muscle, in which M2 macrophage subset was expressed as a percentage of total macrophages (gated as $F4/80^{pos}$ cells) 2 days after injury. Results are means ± s.e.m. of at least 3 independent experiments. *$p<0.05$ $AMPK\alpha1^{-/-}$ *vs.* WT. Bar = 50 µm.

Figure 7 – AMPKα1, CaMKKβ, phagocytosis and macrophage polarization. (A) WT and $AMPK\alpha1^{-/-}$ BMDM were polarized as in Fig.3 and were incubated with fluorescent-PKH67-labeled apoptotic MPCs for 6h, then were labeled with anti-F4/80 antibodies. Phagocytosis is expressed as percentage of double positive cells ($F4/80^+PKH67^+$) among $F4/80^+$ cells. The middle panel represents an example of the dot plots gated on $F4/80^+$ cells, the right panel shows an example of apoptosis (Annexin V^+) /necrosis (Annexin V^+/IP^+) in MPC culture. **(B)** M1 macrophages were incubated (grey bars) or not (white bars) with apoptotic MPCs and the expression of M1 and M2 markers was evaluated by immunofluorescence. **(C)** WT BMDM were polarized in the absence or the presence of STO-609, an inhibitor of CaMPKKβ and iNOS and CD206 expression was evaluated by immunofluorescence. **(D)** WT M1 macrophages were incubated with apoptotic MPCs in the absence or the presence of STO-609, and iNOS and CD206 expression was evaluated immunofluorescence. **(E)** Regenerating WT (3 examples on the left) and $AMPK\alpha1^{-/-}$ (1 example on the right) muscle 2 and 7 days after injury was immunolabeled for macrophages (F4/80, red) and phospho-AMPK (green).

Arrows indicate macrophages expressing p-AMPK, arrowheads indicate macrophages negative for p-AMPK. Green arrows show vessels stained for p-AMPK. Results are means ± s.e.m. of at least 3 independent experiments. *p<0.05, **p<0.01 AMPKα1$^{-/-}$ *vs.* WT. $^{\#}$p<0.05, $^{\#\#}$p<0.01, $^{\#\#\#}$p<0.001 *vs.* untreated M1 macrophages. $^{\$}$p<0.05, $^{\$\$}$p<0.01 STO-609 *vs.*DMSO treated cells. $^{£}$p<0.05, $^{££}$p<0.01 $^{£££}$p<0.001 *vs*. untreated cells (NT). Bar= 50 µm.

Figure 1

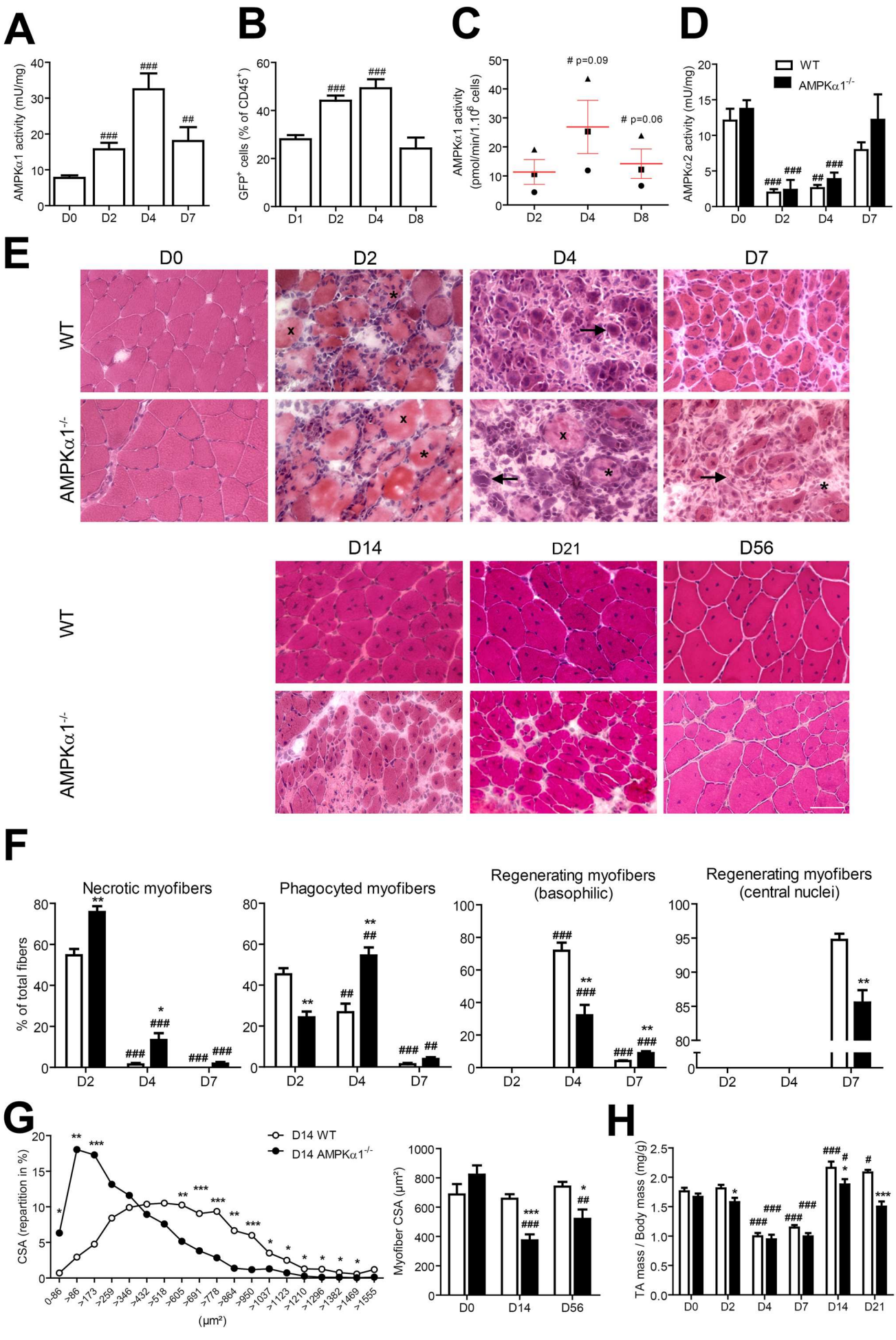
A
AMPKα1 activity (mU/mg)
D0
D2
D4
D7
B
GFP+ cells (% of CD45+)
D1
D2
D4
D8
C
AMPKα1 activity (pmol/min/1.10^6 cells)
p=0.09
p=0.06
D2
D4
D8
D
AMPKα2 activity (mU/mg)
WT
AMPKα1-/-
D0
D2
D4
D7
E
D0
D2
D4
D7
WT
AMPKα1-/-
D14
D21
D56
F
Necrotic myofibers
Phagocyted myofibers
Regenerating myofibers (basophilic)
Regenerating myofibers (central nuclei)
% of total fibers
G
CSA (repartition in %)
D14 WT
D14 AMPKα1-/-
(µm²)
Myofiber CSA (µm²)
H
TA mass / Body mass (mg/g)

Figure 2
Click here to download high resolution image

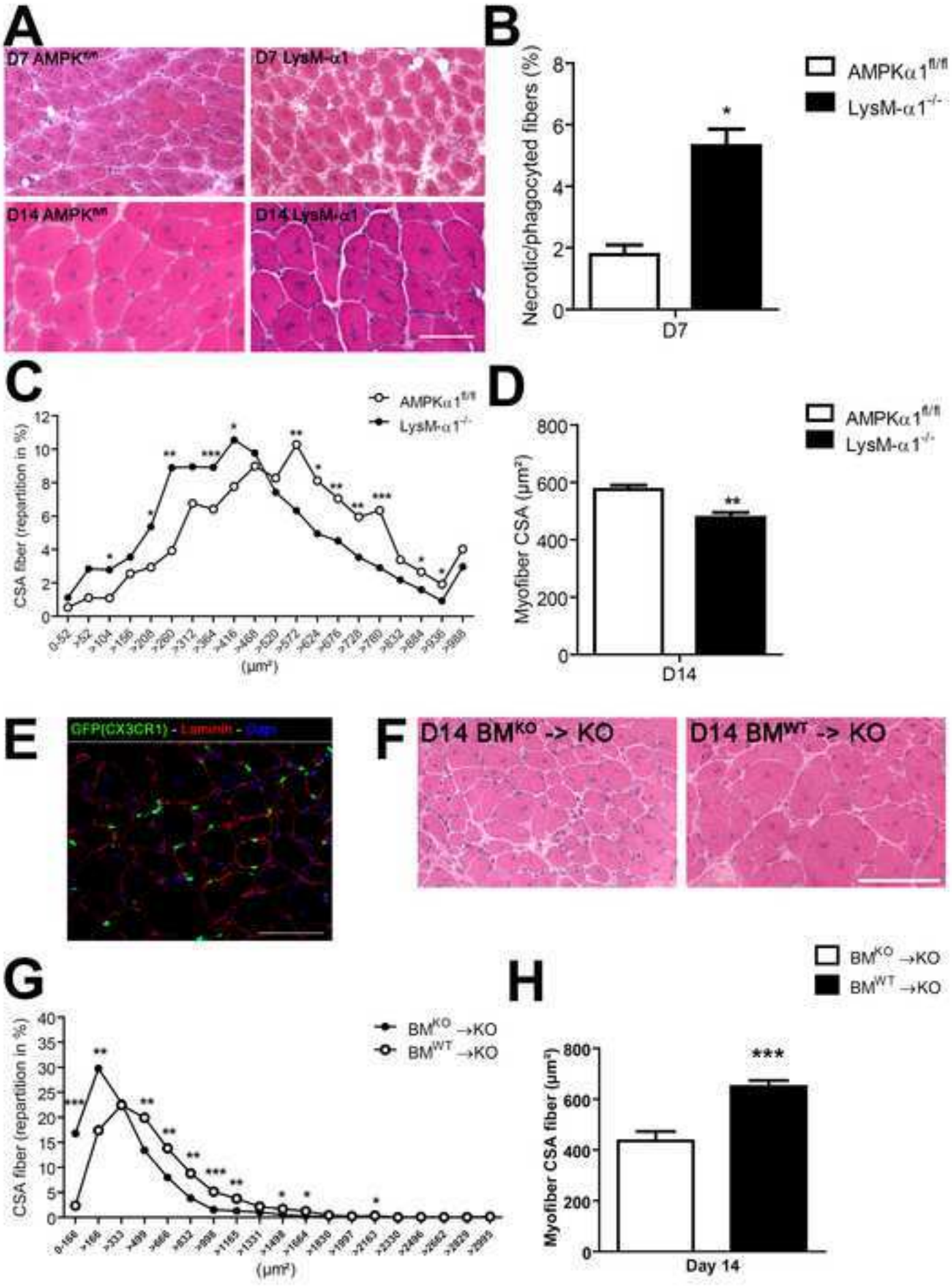

Figure 3

Click here to download high resolution image

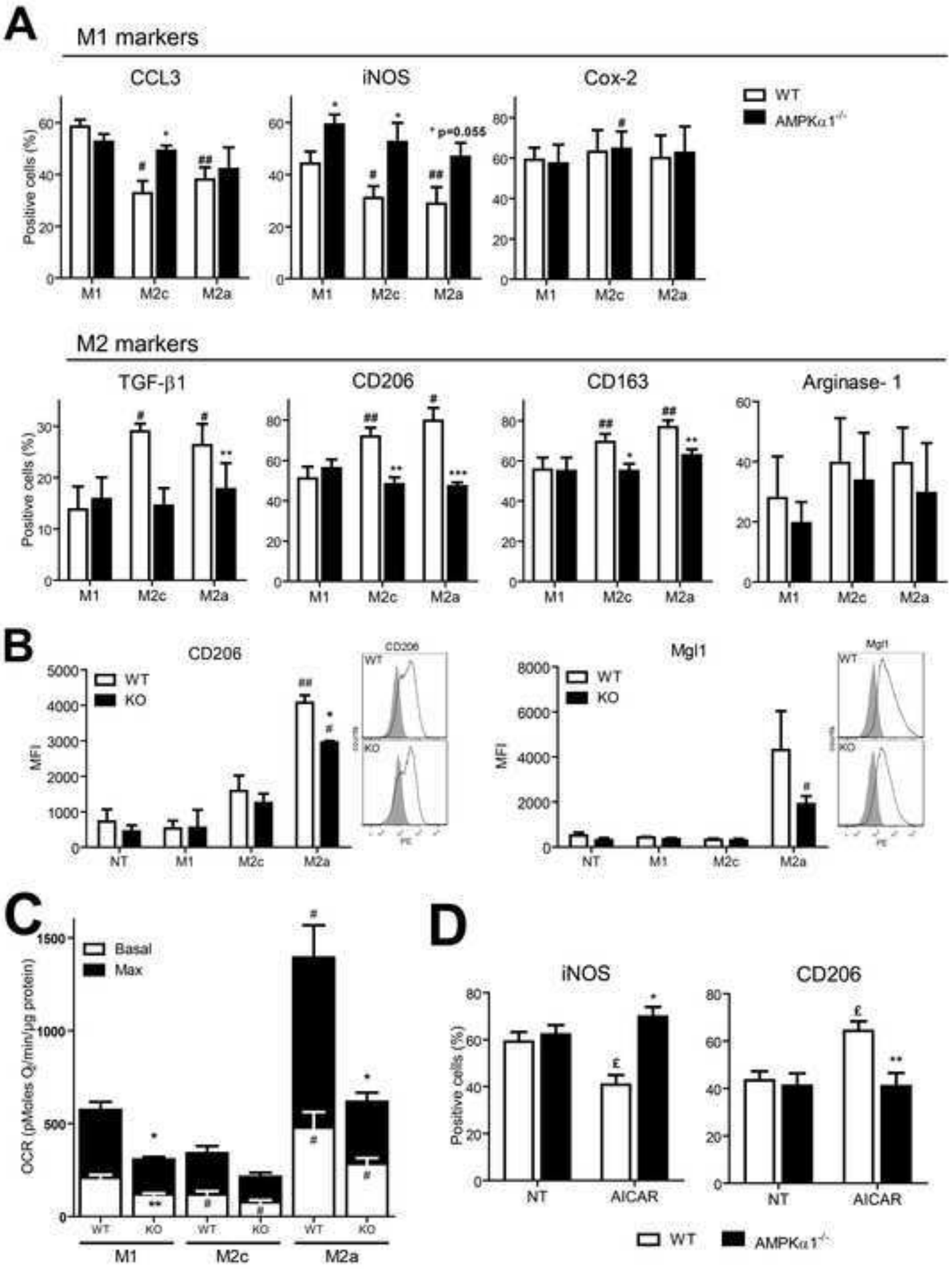

Figure 4
Click here to download high resolution image

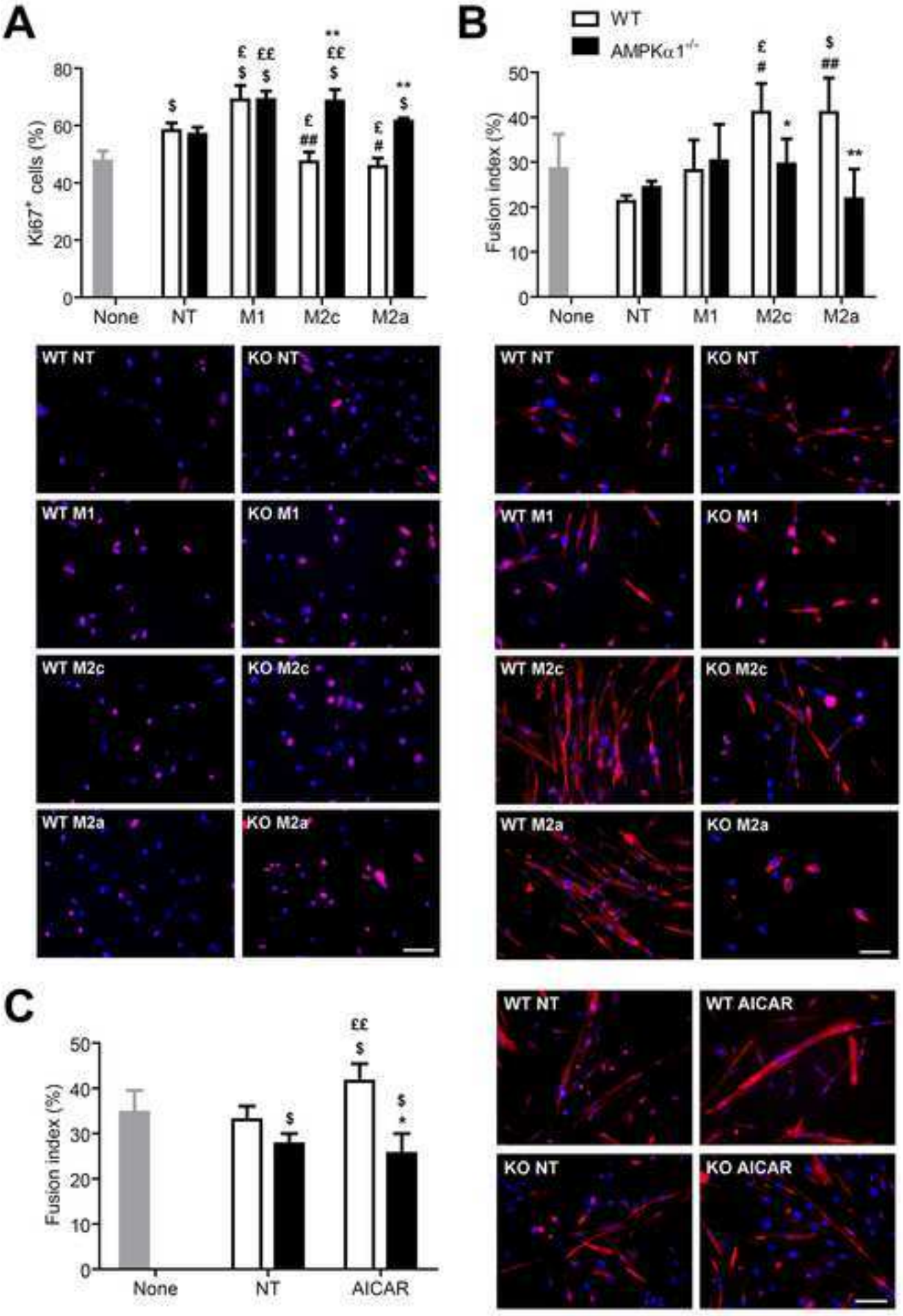

Figure 5
Click here to download high resolution image

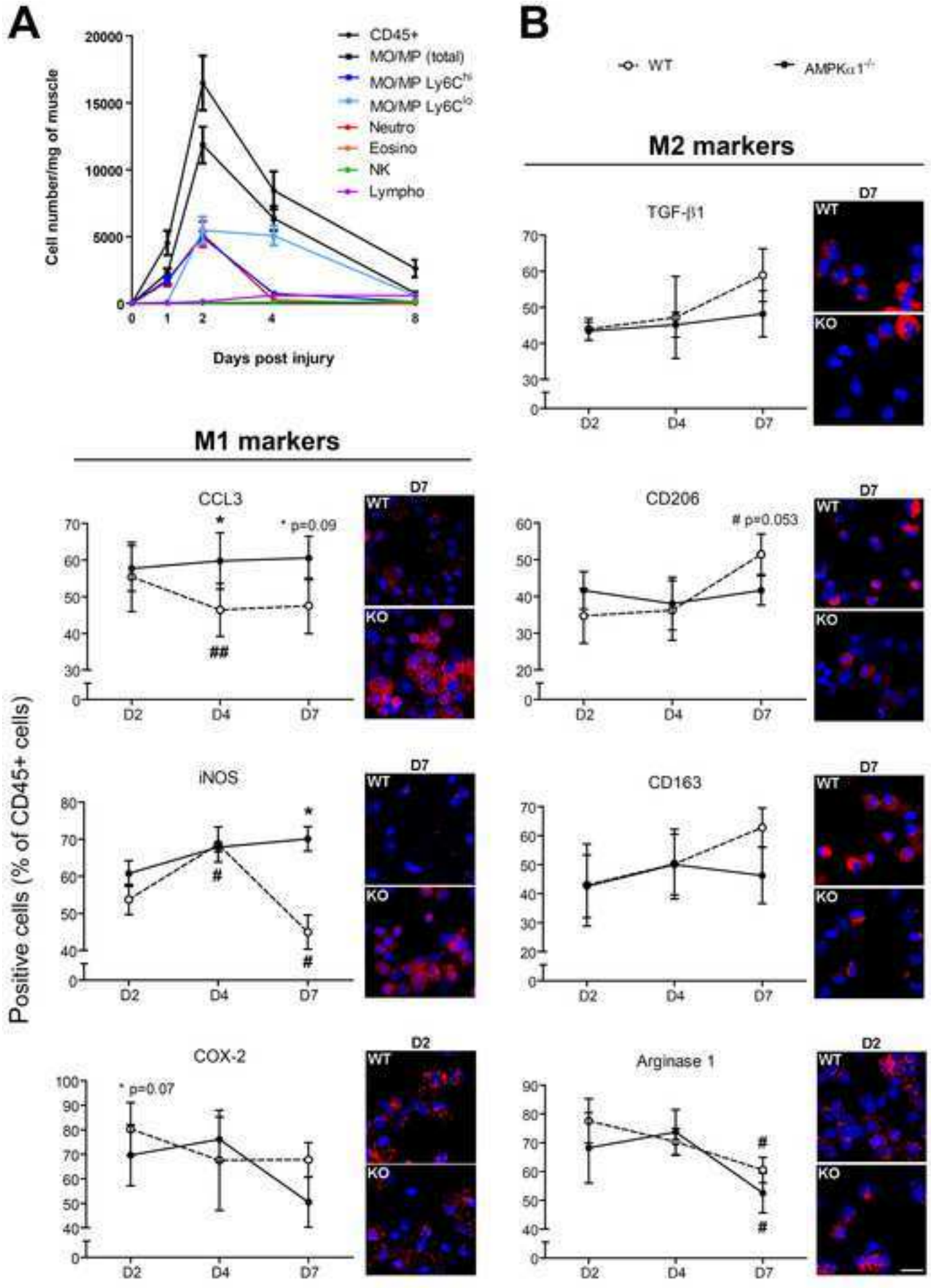

Figure 6
Click here to download high resolution image

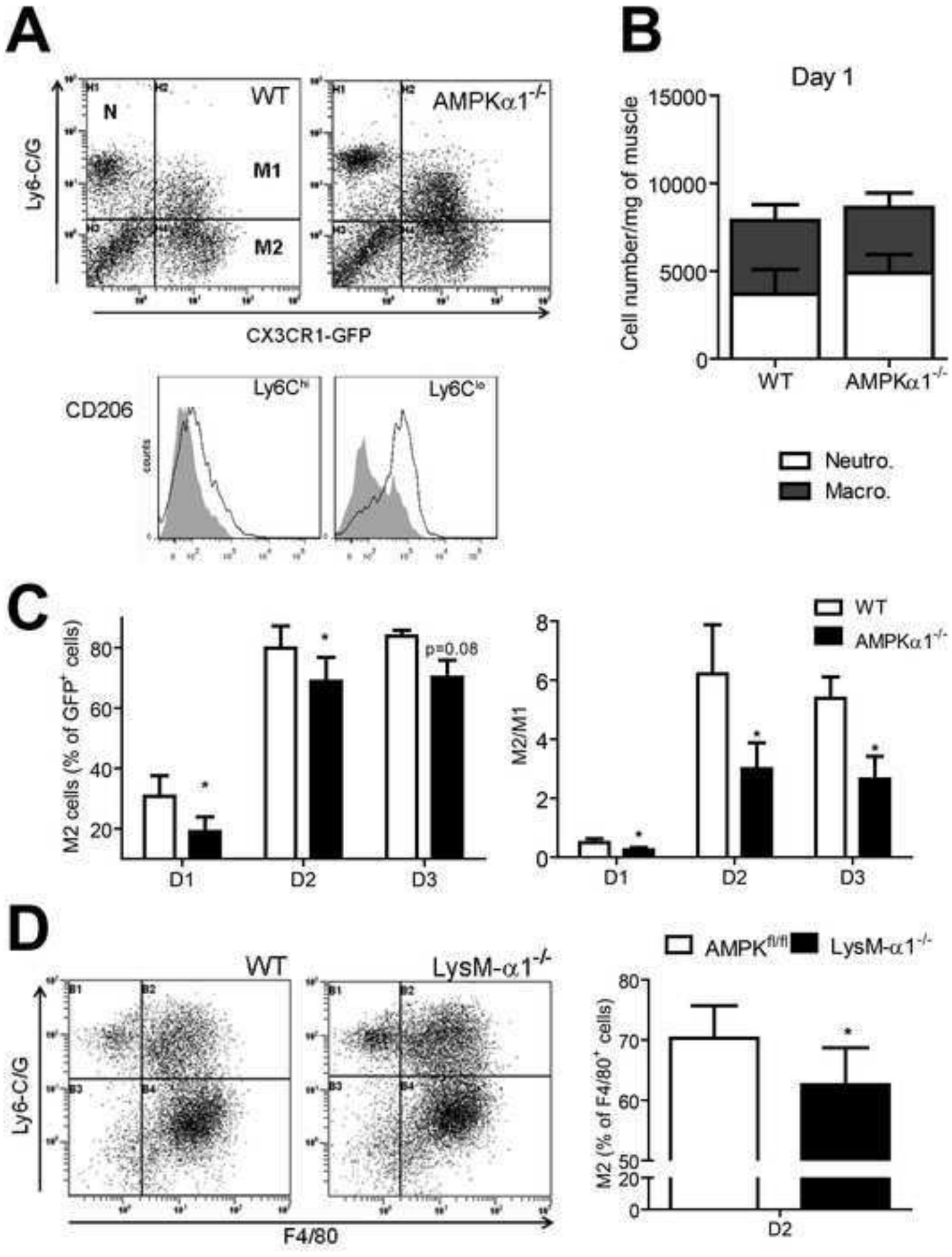

Figure 7

Click here to download high resolution image

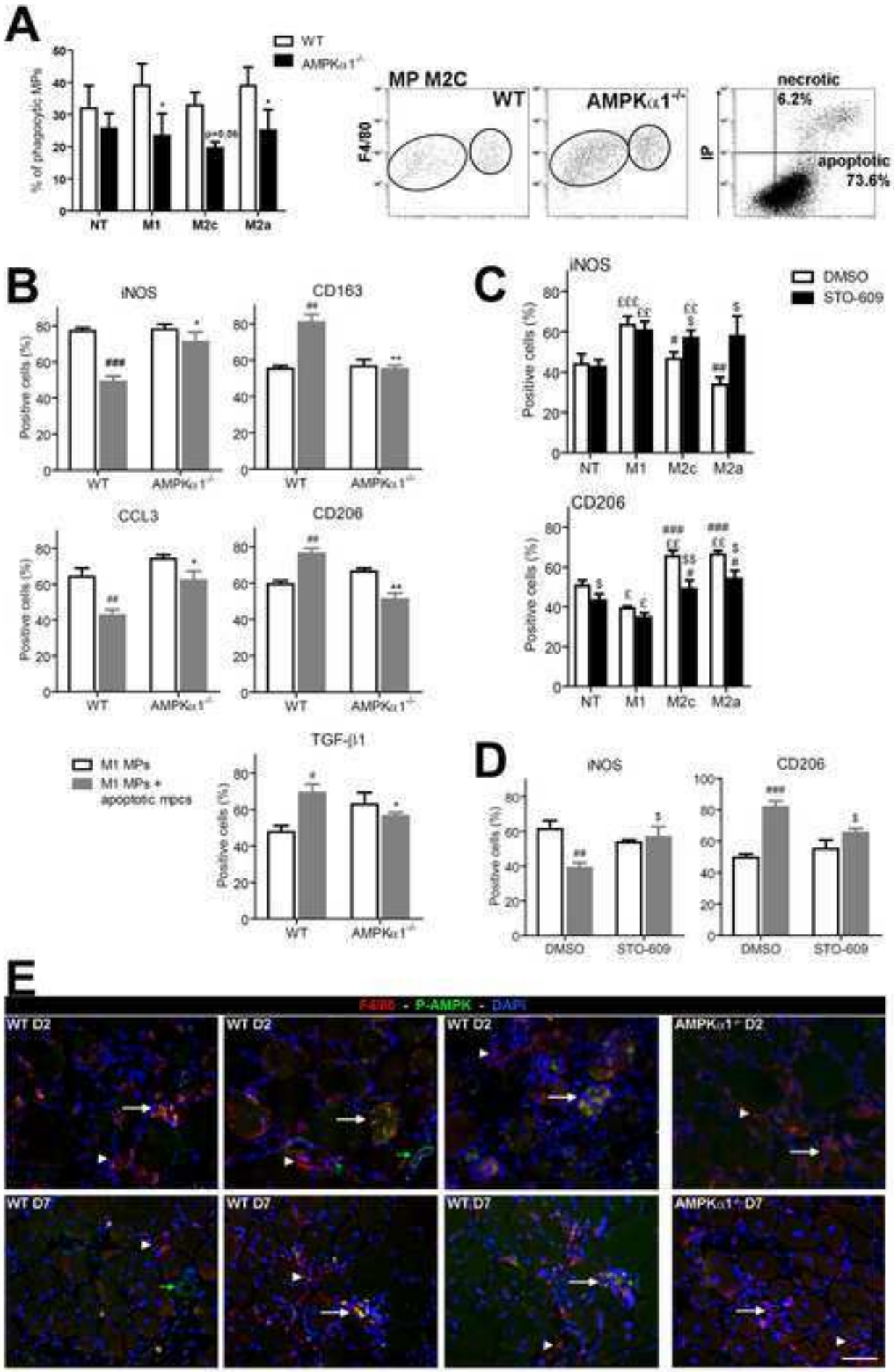

Mounier et al – Supplementary informations

Supplemental figures

- Figure S1 – related to figure 1

Figure S1 completes figure 1 about the model of muscle damage that is used (CTX injection)

- Figure S2 – related to figure 2

Figure S2 described the specificity of deletion of AMPK in conditional mouse strains used in Figure 2

- Figure S3 – related to figure 3

Figure S3 depicts complementary analyses (RT-PCR, illustration of immunolabelings) on macrophage activation performed in Figure 3

- Figure S4 – related to figure 7

Figure S4 shows the absence of effect of upstream kinase activator of AMPK, LKB1.

Supplementary experimental procedures

Supplementary references

Supplementary data

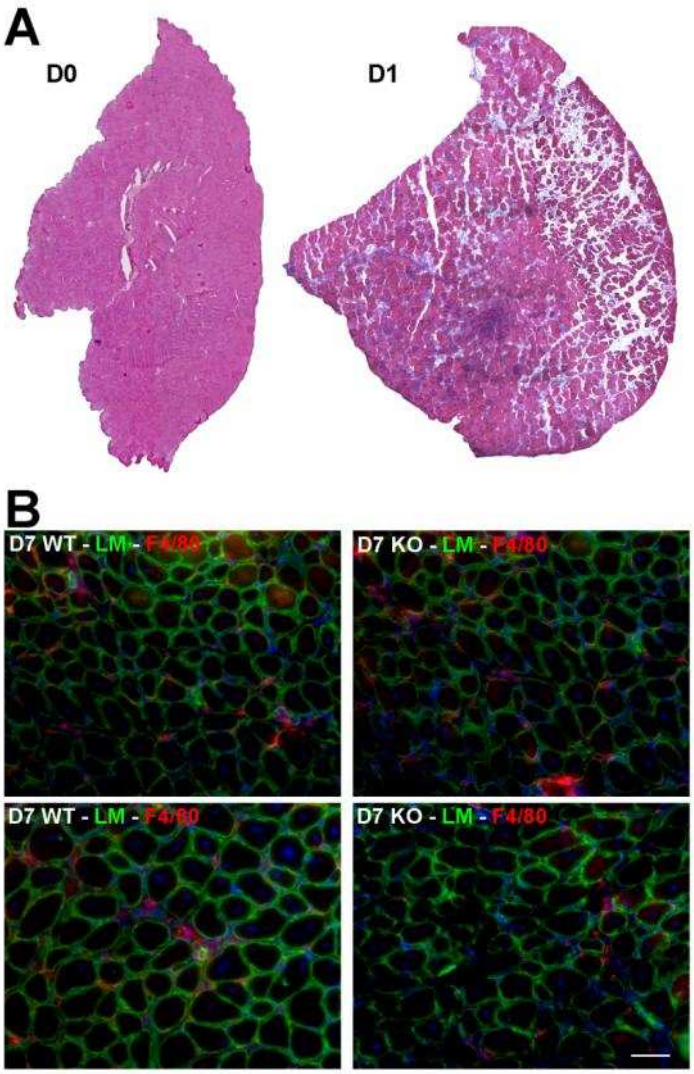

Fig. S1 – Regenerating muscle after cardiotoxin injection. (A) Whole montage of TA muscle before (D0) and at day 1 (D1) after CTX injection showing that the damage triggered by the toxin is homogeneous in the whole muscle. (B) Regenerating muscle at day 7 (D7) after injury was immunolabeled for laminin (green) and macrophages (F4/80, red). Macrophages were still present in the interstitium between growing regenerating myofibers. Bar = 50 µm.

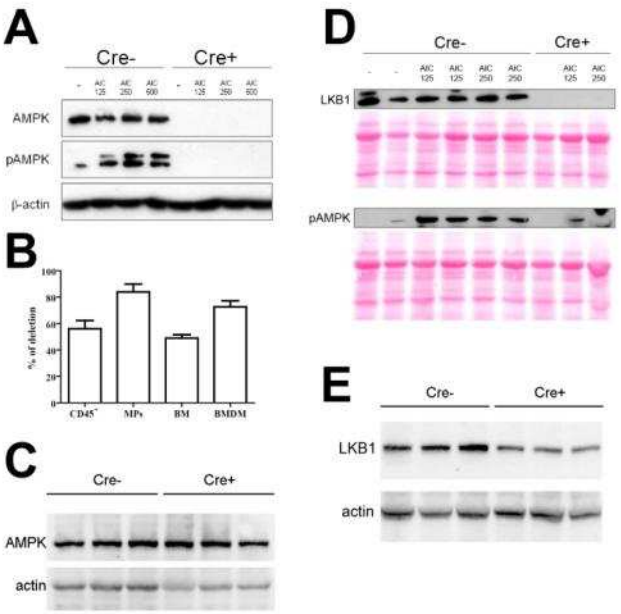

Fig. S2 – Expression of AMPKα1 and LKB1 in macrophages from LysM-α1$^{-/-}$ and LysM-LKB1$^{-/-}$ mice. (A) Peritoneal macrophages were isolated from AMPK$^{fl/fl}$ (Cre-) and LysM-α1$^{-/-}$ (Cre+) mice. Analysis of total AMPK and p-AMPK (T172) levels in the presence or absence of the AMPK activator AICAR was performed by immunoblotting. **(B)** Genomic deletion of AMPKα1 gene in LysM-α1$^{-/-}$ mice was analyzed in total bone marrow (BM), bone marrow-derived macrophages (BMDM), total CD45^{+} cells isolated from regenerating muscle (day 2 post injury) and macrophages (MPs) isolated from the same regenerating muscle. Results are means ± s.e.m. of 3 independent experiments. **(C)** AMPK expression was analyzed by immunoblotting in whole muscle from AMPK$^{fl/fl}$ (Cre-) and LysM-α1$^{-/-}$ (Cre+) muscle (from which fascia was removed). **(D)** Peritoneal macrophages were isolated from LKB1$^{fl/fl}$ (Cre-) and LysM-LKB1$^{-/-}$ (Cre+) mice. Analysis of LKB1 expression in the presence or absence of the AMPK activator AICAR was performed by immunoblotting. **(E)** LKB1 expression was analyzed by immunoblotting in whole muscle from LKB1$^{fl/fk}$ (Cre-) and LysM-LKB1$^{-/-}$ (Cre+) muscle (from which fascia was removed).

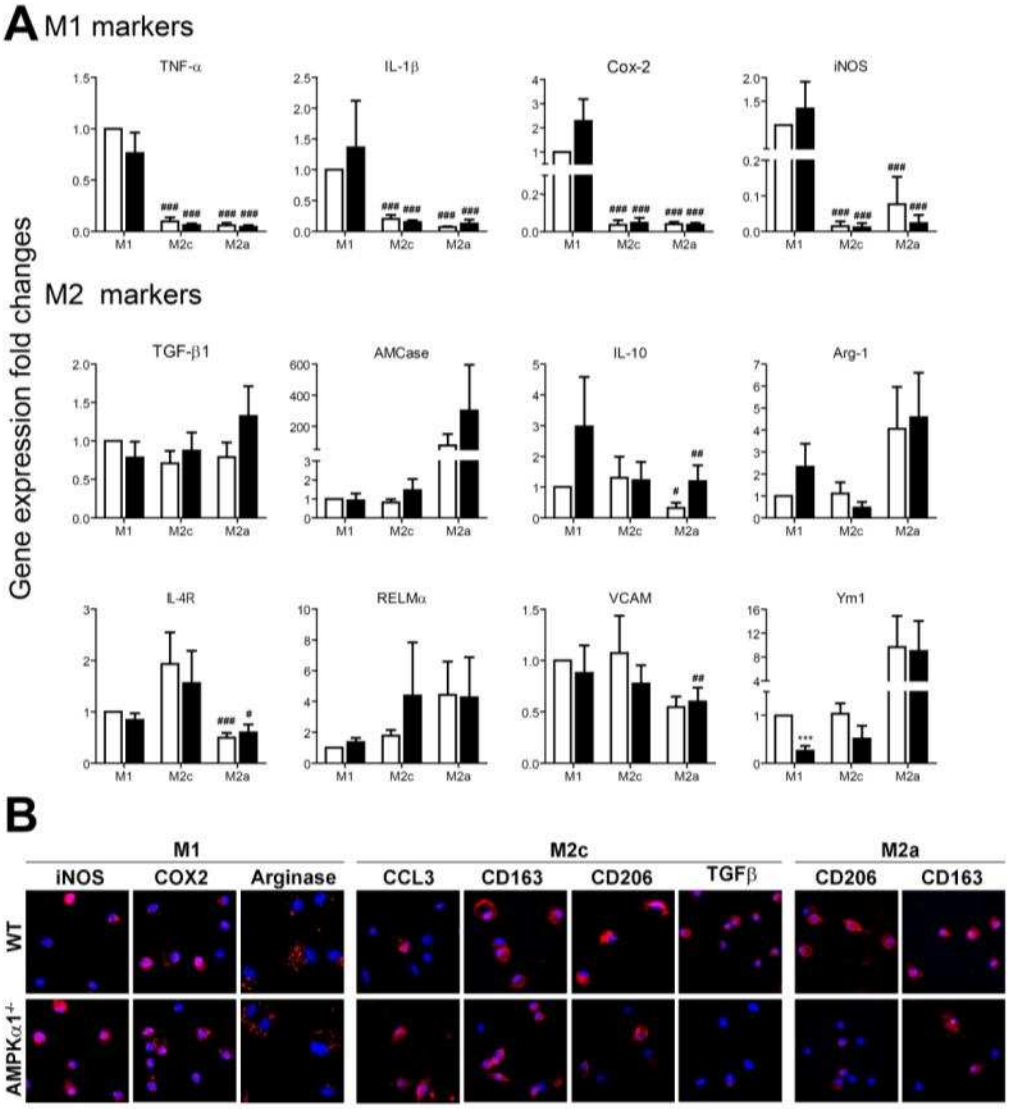

Fig. S3 – Analysis of M1 and M2 markers in WT and AMPKα1$^{-/-}$ macrophages after *in vitro* polarization. WT (white bars) and AMPKα1$^{-/-}$ (black bars) BMDM were polarized as in Fig.3 and were tested for the expression of a series of markers by (A) qRT-PCR and (B) immunoblotting (see quantification in Fig3). Results are means ± s.e.m. of at least 3 independent experiments. ***p<0.001 AMPKα1$^{-/-}$ *vs.* WT; #p<0.05, ##p<0.01, ###p<0.001 *vs.* respective M1.

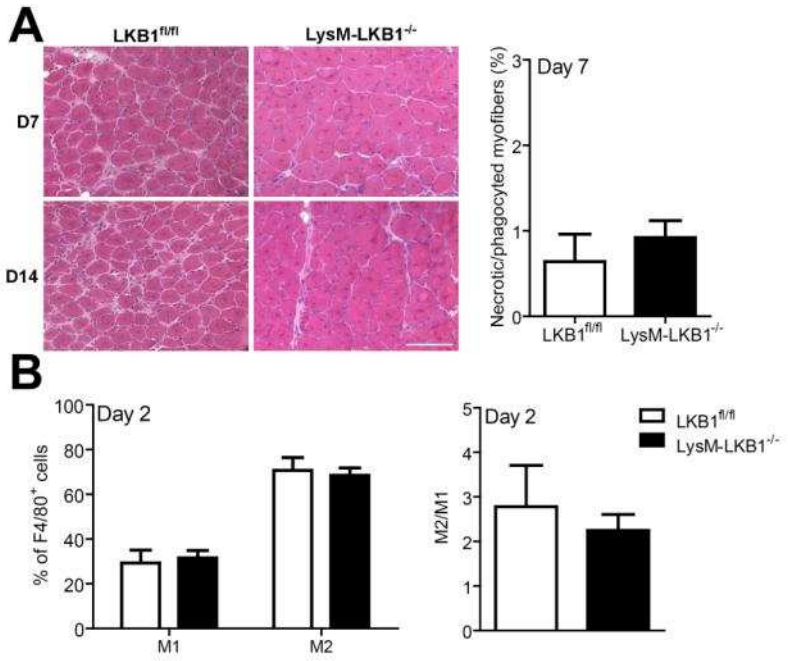

Fig. S4 – Analysis of muscle regeneration and macrophage polarization in LysM-LKB1$^{-/-}$ muscle. (A) HE staining of regenerating muscle at day 7 (D7) and day 14 (D14) in LysM-LKB1$^{-/-}$ and LKB1$^{fl/fl}$ (control), and quantification of necrotic/phagocyted myofibers at day 7. **(B)** The presence of M1 and M2 macrophage subsets was expressed as a percentage of total macrophages (F4/80^{+} cells) in muscle at day 2 after injury. Results are means ± s.e.m. of at least 3 independent experiments. Bar = 50 µm.

Experimental procedures

Mice. Experiments were conducted on adult male animals (8-20 week-old animals) from AMPKα1$^{-/-}$ (Mounier et al., 2009), AMPKα1$^{fl/fl}$ (Miller et al., 2011), LysM-CRE$^{+/-}$:AMPKα1$^{fl/fl}$, CX3CR1$^{GFP/+}$ (Geissmann et al., 2003); CXRCR1$^{GFP/+}$:AMPKα1$^{-/-}$, LysM-CRE$^{+/-}$:LKB1$^{fl/fl}$, LKB1$^{fl/fl}$ (kindly provided by Ron DePinho) (Bardeesy et al., 2002) mouse strains. Mouse strains were bred and experimented in compliance with French and European regulations. Animal facility is fully licensed by French authorities (number A-75-1402). The principal investigator had declared the protocols used in this study and is licensed for these experiments by the local Animal Care and Use Committees of DDPP (Direction Départementale de la Protection des Populations) (number A-75-1506).

Muscle injury. Muscle injury was caused by intramuscular injection of cardiotoxin (CTX), as previsously described (Perdiguero et al., 2011). Mice were anaesthetized with isoflurane and 50 µl of CTX (12.10^{-6} mol/l) was injected in the *tibialis anterior* (TA) muscle. Muscles were harvested for analysis at different time points post-injury (1, 2, 3, 4, 7, 14, 21 and 56 days).

Histological and immunohistochemical analysis. TA muscles were removed, snap frozen in nitrogen-chilled isopentane and kept at –80°C until use. 10 µm-thick cryosections were prepared for hematoxylin-eosin staining or for immunolabeling.

In vivo **immunolabelings.** TA cryosections were treated with antibodies directed against laminin (L9393 sigma), F4/80 (ab6640 abcam), Ki67 (ab15580 abcam) and p-AMPK (2531 Cell signaling), revealed with FITC- or Cy3-conjugated secondary antibodies (Jackson Immunoresearch Inc).

Bone marrow transplantation. Bone marrow (BM) transplantation was performed as previously described (Perdiguero et al., 2011). Donor BM cells were obtained by flushing femurs BM of CX3CR1$^{GFP/+}$ or CXRCR1$^{GFP/+}$:AMPKα1$^{-/-}$ mice with cRPMI medium (Gibco) 10% Foetal Bovine Serum (FBS). Cells were filtered, and counted in cRPMI 25mM Hepes. Retro-orbital injection of 5×10^6 BM cells in 0.1 ml of mouse serum/cRPMI (1:1), was performed in 9.0 Gy-irradiated mice (^{60}Co γ rays 6-8h

prior). After transplantation, mice received ciprofloxacin (10 mg/kg/day) for 2 weeks. Muscle injury was performed 10 weeks after BM transplantation.

Isolation of leukocytes and macrophages from muscle. Fascia of the TA muscles was removed. The muscles were minced and digested in RPMI medium containing collagenase B 0.2% (Roche Diagnostics GmbH) at 37°C for 1 h. The resulting homogenate was filtered, and cells were counted. $CD45^+$ cells were isolated using magnetic sorting (Miltenyi Biotec) and incubated with anti-mouse FcγRII/III (2.4G2) for 10 min à 4°C in FACS buffer (Ca2+/Mg2+-free PBS with 0.5% BSA). Cell were then stained with APC-conjugated anti-Gr1 (Ly6C/G) antibody (eBioscience), anti-F4/80 (ebioscience), anti-CD206 (Biolegend). To evaluated the nature of leukocyte infiltration, cells were stained with the following fluorescent conjugated anti-mouse antibodies from BD Biosciences unless specified: "Myeloid mix": V450-Ly6G, FITC-CD11c, biotinylated anti-Mgl1 (MCA2392B Serotec), PerCP-Cy5.5-CD11b, APC-F4/80 (ebiosciences), PE-Cy7-NK1.1, APC-Cy7-Ly6C; "Lymphocyte mix": PE-CD3, PerCP-Cy5.5-CD8, APC-CD4. Cells were analyzed using a flow cytometer (FC-500; Beckman Coulter) or a FACS Canto II (BD biosciences) using Diva and FlowJo software. Analysis was performed with CXPTM Cytometer. In some experiments, CD45+ cells were cytospined (Cellspin I, Tharmac) on starfrost (Knitterglaser) slides and immunostained (see below). In some experiments, macrophage subsets were sorted using a FACSAria III cell sorter (BD Biosciences).

Macrophage cell culture. Macrophages were obtained from BM precursor cells as previously described (Stanley, 1997). Briefly, total BM was obtained from mice by flushing femurs and tibiae bone marrow with DMEM. Cells were cultured in DMEM medium containing 20% FBS and 30% conditioned medium of L929 cell line (enriched in CSF-1) and prepared as in (Schleicher and Bogdan, 2009)) for 7 days. Purity of differentiated macrophages was estimated by flow cytometry after F4/80-PECy7 labeling (ebiosciences). Macrophages were seeded (at 50000 cell/cm^2 for all experiments excepted for collecting supernatants where they were seeded at 80000 cells/cm^2) and were activated with cytokines to obtain various activation states: IFNγ (50 ng/ml), IL4 (10 ng/ml), IL10 (10 ng/ml) to obtain M1, M2a and M2c macrophages, respectively in DMEM containing 10% FBS medium for 3

days. In some experiments, macrophages were incubated with 1 mM AICAR (Tocris) for 4 h or with 5 µM STO-609 (Tocris) or DMSO for 3 days in DMEM containing 10% FBS medium. After washing steps, DMEM serum-free medium was added for 24 h, recovered and centrifugated to obtain macrophage-conditioned medium, or cells were directly used for various analyses.

Myogenic precursor cell (MPC) culture. Murine MPCs were obtained as previously described (Montarras et al., 2000) from TA muscle and cultured using standard conditions in DMEM/ F12 (Gibco Life Technologies) containing 20% FBS and 2% G/Ultroser (Pall Inc). For proliferation studies, MPCs were seeded at 10000 cell/cm^2 on matrigel (1/10) and incubated for 1 day with MP-conditioned medium + 2.5% FBS. Cells were then incubated with anti-ki67 antibodies (15580 Abcam), which were subsequently visualized using cy3-conjugated secondary antibodies (Jackson Immunoresearch Inc). For differentiation studies, MPCs were seeded at 30000 cell/cm^2 on matrigel (1/10) and incubated for 3 days with macrophage-conditioned medium containing 2% horse serum. Cells were then incubated with anti-desmin antibodies (32362 Abcam), in combination with a cy3-conjugated secondary antibody (Jackson Immunoresearch Inc).

OCR measurement. A Seahorse Bioscience XF96 Extracellular Flux Analyzer (XF96) was used to measure O_2 consumption rate (pmol/min) of BMDMs. Media was replaced with XF assay media (143 mM NaCl, 5.4 mM KCl, 0.8 mM MgSO4, 1.8 mM CaCl2, 0.91 mM NaH2PO4, 15 mg/ml phenol red supplemented with 25 mM glucose, 1 mM sodium pyruvate and 2 mM glutamine) and equilibrated in CO_2–free incubator for 1 h. After baseline measurements of OCR, maximal OCR was measured after sequential injection of oligomycin (1 µg/ml) and CCCP (carbonylcyanide m-chlorophenylhydrazone) (2.5 µM). After measurement of OCR, cells were lysed and protein concentration was determined with the BCA method for normalization.

AMPK activity. Whole skeletal muscle tissue or MPs (freshly-isolated or cultured) were homogenized in lysis buffer as previously described (Sakamoto et al., 2006). AMPK complexes were immunoprecipitated from 50 µg of lysate (muscle tissue) or 200.000 MPs using 1 µg of anti-AMPKα1 or α2 antibody (kind gift from D. Grahame Hardie, University of Dundee, Scotland, UK) and its

phosphotransferase activity was determined toward AMARA peptide (AMARAASAAALARRR) as previously described (Hunter et al. 2011).

***In vitro* immunolabelings.** Macrophages cultured on coverslips or cytospined after muscle extraction were labeled with primary antibodies against the following proteins: CCL3 (sc-1383 Santa-cruz), COX2 (ab2372 Abcam), iNOS (ab3523 Abcam), CD206 (sc-58987 Santa Cruz), CD163 (sc-33560 Santa-cruz), TGFβ1 (ab64715 Abcam), Arginase 1 (sc-18355 Santa Cruz), revealed with a cy3-conjugated secondary antibody (Jackson Immunoresearch Inc). In some experiments, cells were recovered and stained with anti-CD206-PE (Biolegend) and anti-Mgl1-PE (Serotec) and analyzed with a with FACS CANTO II cytometers (BD Biosciences).

Phagocytosis assay. MPCs were labeled with PKH67 (Sigma Aldrich) according to the manufacturer instructions, plated and cultured overnight. MPCs were then treated with staurosporin at 5 µM for 4 h. This leads to apoptosis of myogenic cells (Sonnet et al., 2006). Apoptosis/necrosis was evaluated with Annexin-V-FLUOS staining kit (Roche). Activated macrophages were incubated with apoptotic MPCs at a 1:5 ratio for 30 min at 4°C or 6 h at 37°C. After 5-6 PBS washings, cultures were trypsinized, cells were labeled with F4/80-PeCy7 antibody (ebiosciences) and analyzed by flow cytometry (FC-500; Beckman Coulter). The double positive cells ($F4/80^{pos}PKH67^{pos}$) cells were phagocytic macrophages while the $F4/80^{pos}PKH67^{neg}$ cells were non-phagocytic macrophages. To exclude macrophages that have bound but not ingested apoptotic cells, the percentage of double positive cells observed at 4°C (binding occurs but not endocytosis) was substracted from the value observed at 37°C. To analyze macrophage phenotype, phagocytosis was performed for 6 h as described above with unlabeled apoptotic MPCs. After phagocytosis, macrophages were washed and further cultured in DMEM containing 10% FBS medium for 24 h before immunolabeling was performed as described above. In some experiments, 5 µM STO-609 (or DMSO) was added at the time of phagocytosis.

Image capture and analysis. HE-stained muscle sections were recorded with a Nikon E800 microscope at 20X magnification connected to a QIMAGING camera. For each condition of each

experiment, 8 ± 1 fields chosen randomly in the entire injured area were counted, representing 508 ± 34 myofibers. Quantitative analysis of muscle regeneration was performed using the Image J software and was expressed as a percentage of the total number of myofibers. Necrotic myofibers were defined as pink pale patchy fibers, phagocyted myofibers were defined as pink pale fibers invaded by basophilic single cells (macrophages), regenerating basophilic myofibers were defined as small regenerating myofibers with a basophilic violet cytoplasm and a large central nucleus, regenerating with centrally nuclei myofibers were defined as myofibers presenting one or more centrally located nuclei. CSA of regenerating myofibers was quantified using the Metamorph software (Molecular Devices) and was expressed in arbitrary units. Fluorescent immunolabelings were recorded with a DMRA2 Leica microscope connected to a Coolsnap cf camera at 20X and 40X magnifications (BMDM 20X; $CD45^+$ muscle cells 40X; MPCs 20X). For each condition of each experiment, 9 ± 1 fields chosen randomly were counted, representing a mean of 292 ± 32 cells. The number of labeled macrophages was calculated using the Image J software and expressed as a percentage of total cells. Fusion index (for myogenic cells) was calculated as the number of nuclei within myotubes divided by the total number of nuclei, nuclei number being estimated using the Image J software.

Peritoneal macrophages. Mouse peritoneal macrophages were harvested 3 days following *i.p*. injection of 1 mg zymosan A from *Saccharomyces cerevisiae* (Sigma) by washing the peritoneal cavity with 2-5 ml of cold PBS, 3 mM EDTA, 25 U/ml heparin. The purity of the macrophage population was evaluated by flow cytometry ($F4/80^+$ cells) and was more than 75%. Cells were seeded in 12-well tissue culture plates (10^6 cells/well) in DMEM medium supplemented with 10% FBS, allowed to adhere for 1 h at 37°C and non-adherent cells were removed. Cells were treated with 5-amino-1-β-D-ribofuranosyl-imidazole-4-carboxamide (AICAR) for 4 h.

Western Blot. Total protein extracts from TA muscle (from which the fascia has been removed) or from peritoneal macropahes prepared as above were obtained using Mammalian Cell Lysis Kit (Sigma). Fifty micrograms of protein were subjected to SDS-PAGE and transferred to nitrocellulose

membrane. Blots were probed with antibodies against AMPKα1, kindly provided by Prof. D.G. Hardie (Dundee University, Scotland) as described previously (Foretz et al., 2010) and LKB1 (Cell Signaling), and with a beta-actin antibody for loading control.

qRT-PCR. Total RNAs were extracted using the RNeasy Mini Kit (QIAGEN). 1 µg of total RNA was reverse-transcribed using Superscript II Reverse Transcriptase (Invitrogen). qPCR was carried out on LightCycler® 480 Real-Time PCR System (Roche Applied Science). Reaction mixtures had a final volume of 20 µl, consisting of 3 µl of cDNA, 10 µl of LightCycler® 480 SYBR Green I Master, and 10 µM of primers. After initial denaturation, amplification was performed at 95°C (10 s) 60°C (5 s) 72°C (10 s) for 45 cycles. Calculation of relative expression was determined by the LightCycler® 480 software and fold change was normalized against cyclophilin, a housekeeping gene.

qRT-PCR. Primers:

Arg1 forward AGCTCCAAGCCAAAGTCCTTAGA, *Arg1* reverse CCTCCTCGAGGCTGTCCTT

ptgs2 forward ACTGGGCCATGGAGTGGACTTAAA, *ptgs2* reverse AACTGCAGGTTCTCAGGGATGTGA

Retnla forward CCCTGCTGGGATGACTGCTA, *Retnla* reverse TGCAAGTATCTCCACTCTGGATCT

il10 forward TGAATTCCCTGGGTGAGAAGCTGA, *il10* reverse TGGCCTTGTAGACACCTTGGTCTT

il1b forward GATGAAGGGCTGCTTCCAAAC, *il1b* reverse GTGCTGCTGCGAGATTTGAA

il4ra forward CCTCTGTGGGCTGTCTGATTTT, *il4ra* reverse GGGCTCACCCAGGACCTT

Nos forward CCACCAACAATGGCAACATCAGGT, *Nos* reverse TAGGTCGATGCACAACTGGGTGAA

tnf forward AATGGCCTCCCTCTCATCAGTT, *tnf* reverse CGAATTTTGAGAAGATGATCTGAGTGT

tgfb1 forward AACAACGCCATCTATGAGAAAACC, *tgfb1* reverse CCGAATGTCTGACGTATTGAAGAA

Chi3l3 forward TGCGTGACTATGAAGCATTGAAT, *chi3l3* reverse CCAATGGCCAGGAGAGTTTTT

Vcam1 forward GTGAAGATGGTCGCGGTCTT, *Vcam1* reverse AAGCTTGAGAGACTGCAAACAGTATC

Chia forward ATGGCCAAGCTACTTCTCGTCACA, *Chia* reverse TCCCAGCAAAGGCATAGATCAGGT).

PCR for AMPK deletion. LysM-CRE:AMPKα1$^{fl/fl}$ mice were analyzed for the specific deletion in macrophages. Genomic DNA of total BM, BM-derived macrophages, total leukocytes and macrophages sorted from regenerating muscle was extracted as followed. Cells were lysed in 100

mM Tris (pH 8.5), 5 mM EDTA (pH 8.0), 200 mM NaCl, 0.2% SDS, 0.1 mg/ml proteinase K (Roche) lysis buffer for 2 h at 55°C. DNA was precipitated with isopropanol and glycogen, washed with ethanol, dried and solubilized in water. PCR was performed using Phire® Hot Start II DNA Polymerase (Finnzymes) with 100ng of genomic DNA. After initial denaturation 30s at 98°C, amplification was performed at 98°C (7 s) 62°C (10 s) 72°C (1m) for 35 cycles, final elongation for 30s at 72°C. Primers sequences were ampka1Lox5 : attaaacaccactaattggaaaacattccc, ampka1Lox33 : gacctgacagaataggatat gcccaacctc. The degree of excision was given in percentages of the amount of the floxed allele compared to that of the intact allele, after quantification with Image J software.

Statistical analyses. All experiments were performed using at least three independent primary cultures or at least 5 animals for *in vivo* analyses. Isolation of macrophages from regenerating muscle required for each experiment, 3, 2, 5 mice at 2, 4 and 7 days after injury, respectively. Depending of the experiments, the Student's t-test or two-way ANOVA test was performed and Bonferroni post-tests were applied. $P<0.05$ was considered significant.

Reference List

Bardeesy, N., Sinha, M., Hezel, A.F., Signoretti, S., Hathaway, N.A., Sharpless, N.E., Loda, M., Carrasco, D.R., and DePinho, R.A. (2002). Loss of the Lkb1 tumour suppressor provokes intestinal polyposis but resistance to transformation. Nature *419*, 162-167.

Foretz, M., Hebrard, S., Leclerc, J., Zarrinpashneh, E., Soty, M., Mithieux, G., Sakamoto, K., Andreelli, F., and Viollet, B. (2010). Metformin inhibits hepatic gluconeogenesis in mice independently of the LKB1/AMPK pathway via a decrease in hepatic energy state. J Clin. Invest *120*, 2355-2369.

Geissmann, F., Jung, S., and Littman, D.R. (2003). Blood monocytes consist of two principal subsets with distinct migratory properties. Immunity *19*, 71-82.

Miller, R.A., Chu, Q., Le, L.J., Scherer, P.E., Ahima, R.S., Kaestner, K.H., Foretz, M., Viollet, B., and Birnbaum, M.J. (2011). Adiponectin suppresses gluconeogenic gene expression in mouse hepatocytes independent of LKB1-AMPK signaling. J Clin. Invest *121*, 2518-2528.

Montarras, D., Lindon, C., Pinset, C., and Domeyne, P. (2000). Cultured myf5 null and myoD null muscle precursor cells display distinct growth defects. Biol. Cell *92*, 565-572.

Mounier, R., Lantier, L., Leclerc, J., Sotiropoulos, A., Pende, M., Daegelen, D., Sakamoto, K., Foretz, M., and Viollet, B. (2009). Important role for AMPK{alpha}1 in limiting skeletal muscle cell hypertrophy. FASEB J. *23*, 2264-2273.

Perdiguero, E., Sousa-Victor, P., Ruiz-Bonilla, V., Jardi, M., Caelles, C., Serrano, A.L., and Munoz-Canoves, P. (2011). p38/MKP-1-regulated AKT coordinates macrophage transitions and resolution of inflammation during tissue repair. J. Cell Biol. *195*, 307-322.

Sakamoto, K., Zarrinpashneh, E., Budas, G.R., Pouleur, A.C., Dutta, A., Prescott, A.R., Vanoverschelde, J.L., Ashworth, A., Jovanovic, A., Alessi, D.R., et al (2006). Deficiency of LKB1 in heart prevents ischemia-mediated activation of AMPKalpha2 but not AMPKalpha1. Am J Physiol Endocrinol. Metab *290*, E780-E788.

Schleicher, U. and Bogdan, C. (2009). Generation, culture and flow-cytometric characterization of primary mouse macrophages. Methods Mol Biol *531*, 203-224.

Sonnet, C., Lafuste, P., Arnold, L., Brigitte, M., Poron, F., Authier, F.J., Chretien, F., Gherardi, R.K., and Chazaud, B. (2006). Human macrophages rescue myoblasts and myotubes from apoptosis through a set of adhesion molecular systems. J. Cell Sci. *119*, 2497-2507.

Stanley, E.R. (1997). Murine bone marrow-derived macrophages. Methods Mol. Biol. *75*, 301-304.